

**EXPLORATION OF THE FUNCTION OF A NON-PROLYL CIS-PEPTIDE
BOND IN HUMAN PLASMA PLATELET-ACTIVATING FACTOR
ACETYLHYDROLASE**

by

Shilin Xie

A thesis submitted to the Faculty of the University of Delaware in partial fulfillment of the requirements for the degree of Master of Science in Chemistry and Biochemistry

Summer 2017

© 2017 Shilin Xie
All Rights Reserved

**EXPLORATION OF THE FUNCTION OF A NON-PROLYL CIS-PEPTIDE
BOND IN HUMAN PLASMA PLATELET-ACTIVATING FACTOR
ACETYLHYDROLASE**

by

Shilin Xie

Approved:

Brian J. Bahnsen, Ph.D.
Professor in charge of thesis on behalf of the Advisory Committee

Approved:

Murray V. Johnston, Ph.D.
Chair of the Department of Chemistry & Biochemistry

Approved:

George H. Watson, Ph.D.
Dean of the College of Arts and Sciences

Approved:

Ann L. Ardis, Ph.D.
Senior Vice Provost for Graduate and Professional Education

ACKNOWLEDGMENTS

I would have never had the opportunity to pursue a graduate degree and finish this thesis without the support from numerous people around me. I would like to take a moment to thank some of these people.

First and foremost, I would like to thank my advisor, Dr. Brian Bahnsen. When I started my degree I lacked a strong background in biochemistry and was not confident in my abilities to do independent research. But you still gave me a chance to perform this research in your lab. I truly appreciate that you have shown great patience guiding me through my inadequacies during the past three years.

I would also like to thank my labmates, both past and present. Thank you Kaitlyn Worner, for helping to train me in techniques I would need and for passing off your project to me before you left. Thank you Dr. Tara Gonzalez, for giving me great courage to express what I was thinking when I first came here and to feel less nervous about my new circumstances. Thank you Dr. Meghan Klems, for answering any questions I had and your willingness to offer me help whenever I needed. Thank you Dr. Mackenzie Lauro, for your kindness and great help when you were also struggling to finish your dissertation and apply for jobs. Thank you to the current lab member Walter Drake, you've been a great help for teaching me nearly all the experimental protocols and showing great patience on my endless questions. I also want to thank Michael Willburn, who directed the way of crystallization and molecular dynamics patiently while you are occupied by your work and academic study at the same time.

Besides the great help I received at the University of Delaware, I would like to thank my parents for all their support. Thank you mom and dad! I would have never completed this goal if you did not encourage me to pursue a degree in another country far away from China. You always stood by me through many obstacles and setbacks and gave me positive reinforcement for my efforts. I feel heartily grateful to be your daughter.

TABLE OF CONTENTS

LIST OF TABLES	vii
LIST OF FIGURES.....	viii
LIST OF ABRREVIATION.....	x
ABSTRACT	xii
Chapter	
1 INTRODUCTION.....	1
1.1 Cis Peptide Bonds in Protein.....	1
1.2 Platelet-Activating Factor Acetylhydrolase (PAF-AH)	6
1.3 Non-Prolyl Cis Peptide Bond in Plasma PAF-AH	10
REFERENCES	17
2 MOLECULAR CLONING AND MUTAGENESIS OF ΔPAF-AH	23
2.1 Introduction	23
2.2 Materials and Methods	24
2.2.1 Materials	24
2.2.2 Molecular cloning of ΔPAF-AH	24
2.2.3 Mutagenesis of ΔPAF-AH.....	26
2.2.3.1 D73P	26
2.2.3.2 D73G	27
2.3 Results and Discussion	29
2.4 Conlusions	30
REFERENCES	31
3 EXPRESSION AND PURIFICATION OF PAF-AH.....	32
3.1 Introduction	32
3.2 Materials and Methods	33
3.2.1 Materials	33

3.2.2	Expression of ΔPAF-AH and mutants in E.coli	34
3.2.3	Purification of ΔPAF-AH and mutants.....	34
3.2.3.1	Protein affinity chromatography.....	34
3.2.3.2	Q-sepharose anion exchange chromatography	36
3.2.3.3	Size-exclusion chromatography	37
3.2.4	Purification of PreScission Protease.....	37
3.2.5	BCA Assay	38
3.2.6	PNPA activity assay	38
3.3	Results and Discussion	40
3.3.1	Expression and purification of ΔPAF-AH and mutants	40
3.3.2	PNPA assay	48
3.4	Conclusions	49
	REFERENCES	51
4	CIRCULAR DICHROISM CHARACTERIZATION OF ΔPAF-AH AND CIS-PEPTIDE BOND MUTANT STABILITY	52
4.1	Introduction	52
4.2	Methods and Materials	54
4.2.1	Materials	54
4.2.2	Determination of secondary structure of ΔPAF-AH	54
4.2.3	Circular dichroism thermodynamics determination of melting temperature of ΔPAF-AH	55
4.3	Results and Discussions	56
4.3.1	Secondary structural analysis	56
4.3.2	Determination of melting temperature	58
4.4	Conclusions	62
5	CONCLUSION AND FUTURE DIRECTION.....	65
	Appendix	
	PERMISSION LETTER	67

LIST OF TABLES

Table 1.1:	Amino acids predicted for lipoprotein binding in plasma PAF-AH	13
Table 3.1:	Predicted pI for Δ PAF-AH and cis-peptide bond mutants	33
Table 3.2:	Yield and purity of protein samples of Δ PAF-AH, D73G and D73P	50
Table 4.1:	Protein yield, purity and melting temperature.....	63

LIST OF FIGURES

Figure 1.1: Trans and cis conformation of peptide bonds	1
Figure 1.2: Cis-trans isomerization of a prolyl peptide bond.	2
Figure 1.3: Non-proline and proline peptide fragments in trans and cis conformations.	4
Figure 1.4: Function of cis peptide bond in protein.	5
Figure 1.5: PAF-AH catalyzes the hydrolysis of PAF.	6
Figure 1.6: Structure of plasma PAF-AH.....	8
Figure 1.7: Stick diagram of Phe-72 and Asp-73 in plasma PAF-AH.	11
Figure 1.8: Orientation of PAF-AH on a membrane surface, predicted by OPM.	13
Figure 1.9: Acidic and basic patches in PAF-AH..	14
Figure 1.10: Sequencing alignment result of plasma PAF-AH from mammals.....	15
Figure 1.11 Stick diagram of Mutagenesis in PAF-AH	16
Figure 2.1: The PCR parameter for the amplification of Δ PAF-AH in pGEX-6P1 vector.....	25
Figure 2.2: The PCR parameter for the mutation of D73P.....	26
Figure 2.3: The PCR parameter for the mutation of D73G.	28
Figure 2.4: Sequencing alignment results.....	29
Figure 3.1 PAF-AH hydrolyze PNPA to p-nitrophenoxide and acetate.....	39
Figure 3.2: SDS PAGE for the cells expression.	41
Figure 3.3: SDS PAGE for wild type Δ PAF-AH after first purification.	42
Figure 3.4: SDS PAGE for wild type Δ PAF-AH after second purification.	43

Figure 3.5: SDS PAGE for cis-peptide bond mutant D73G after first purification ..	44
Figure 3.6: SDS PAGE for cis-peptide bond mutant D73G after second purification	45
Figure 3.7: SDS PAGE for cis-peptide bond mutant D73P after first purification ...	46
Figure 3.8: SDS PAGE for cis-peptide bond mutant D73P after second purification	47
Figure 3.9: Specific enzyme activity of Δ PAF-AH and cis-peptide bond mutants ..	49
Figure 4.1: Characteristic circular dichroism spectra of secondary structure of protein.....	53
Figure 4.2: Circular dichroism secondary structure analysis.. ..	57
Figure 4.3: (A) Sample curve of sigmoid curve vs. Boltzmann function (B) Formula of sigmoid curve vs. Boltzmann function	58
Figure 4.4: Circular dichroism thermodynamics analysis of Δ PAF-AH.....	59
Figure 4.5: Circular dichroism thermodynamics analysis of cis-peptide mutant D73P	60
Figure 4.6: Circular dichroism thermodynamics analysis of cis-peptide mutant D73G	61

LIST OF ABRREVIATION

apoB100	Apolipoprotein B100
ATP	Adenosine-5'-triphosphate
BCA	Bicinchoninic acid
BSA	Bovine serum albumin
CD	Circular Dichroism
CHD	Coronary heart diseases
CVD	Cardiovascular diseases
DTT	Dithiothreitol
EDTA	Ethylenediamine- <i>N,N,N',N'</i> -tetraacetic acid
GST	Glutathione S-transferase
HDL	High density lipoprotein
IPTG	Isopropyl- β -d-thiogalactopyranoside
LB	Luria-Bertani media
LDL	Low density lipoprotein
Lp-PLA ₂	Lipoprotein-associated phospholipase A ₂
Lyso-PAF	Lyso-platelet activating factor
	1-O-alkyl- <i>sn</i> -glycero-3-phosphocholine
OPM	Orientations of proteins in membranes
PAF	Platelet-activating factor
	1-O-alkyl-2- <i>sn</i> -glycero-3-phosphocholine
PAF-AH	Platelet-activating factor-acetylhydrolase

PAF-AH II	Intracellular type II PAF-AH
PCR	Polymerase chain reaction
pI	Isoelectric point
PNPA	4-Nitro phenylacetate
SDS	Sodium dodecyl sulfate
SDS-PAGE	Sodium dodecyl sulfate-polyacrylamide gel electrophoresis

ABSTRACT

Plasma platelet-activating factor acetylhydrolase (PAF-AH), also known as lipoprotein-associated phospholipase A2, is an extracellular 45 KDa monomer that circulated in plasma and associates with lipoproteins. As a group-VIIA PLA2 enzyme, it catalyzes the hydrolysis of the acetyl group at the sn-2 position of platelet-activating factor (PAF) to form the products lyso-PAF and acetate. Additionally, PAF-AH can hydrolase a wide range of substrates with a short acetyl chain at the sn-2 position like oxidized phospholipids from LDL oxidation. In order to keep PAF-AH constitutively active without undermining cellular integrity, the enzyme only targets oxidatively fragmented phospholipids. A majority of PAF-AH is bound to low-density lipoprotein (LDL), which might be correlated with inflammatory atherogenesis. Studies show that an increase of PAF-AH concentration or activity could possibly lead to an increase in risk of atherogenesis, which plays a significant role in heart diseases. Many reversible PAF-AH inhibitors were developed in the pharmaceutical industry for the use as an extra treatment for patients with heart diseases.

According to the solved structure via x-ray crystallization, there is a rare non-prolyl cis-peptide bond located between Phe-72 and Asp-73, which is far away from the active site catalytic triad formed by Ser-273, Asp-296 and His-351. Due to the high energy barrier of cis-trans isomerization, this conformational change is thought to be the rate-limit step in the protein folding process. Therefore, the existence of a cis-peptide bond usually is thought to play a great role in protein function or enhance structural stability in some way. The purpose of the existence of this non-prolyl cis-

peptide in PAF-AH is still unsolved. Based on the previous work of plasma PAF-AH's cis-peptide bond, a hypothesis was formed that this non-prolyl cis-peptide bond plays a role in maintaining the binding between LDL and PAF-AH.

Work presented in this thesis aims to test this hypothesis. An *E. coli* expression construct of a truncated form of PAF-AH (Δ PAF-AH) was obtained from former lab member from the Bahnsen lab. In an effort to explore the function role of a cis-peptide bond at this position, two site-directed mutants (D73G and D73P) were created at the position of this cis-peptide bond. D73G mutant aims to mimic the mouse PAF-AH that is reported only bound to high density lipoprotein (HDL) and D73P mutant aims to mimic the common prolyl cis-peptide bond. Expression and purification of Δ PAF-AH, as well as cis-peptide bond mutants, were performed using *E. coli* expression construct. Enzyme activity assays using a general substrate were carried out and proved that there were no functional differences between wild type and cis-peptide bond mutants, indicating the cis-peptide bond does not play a role in enzyme activity. Moreover, there are no significant differences of circular dichroism (CD) secondary structure test between wild type and mutants, eliminating the possibility that this cis-peptide bond may have a influence on protein folding. Through CD thermodynamics test, there was a significant decrease of stability of D73G mutant while D73P mutant only show a little decline of stability. Possible explanation is that D73G might have changed this position to a trans configuration, which leads to the instability of protein. In order to test this explanation, high-purity mutant protein samples were produced for further crystallization trials.

Chapter 1

INTRODUCTION

1.1 Cis Peptide Bonds in Protein

Proteins and peptides are known of biological molecules that compose of long chains of amino acids. Amino acids are linked together through their carboxylate carbon and amine nitrogen atoms, which forms peptide bond. With the purpose for interpretation of peptide conformation, three dihedral angles (also known as torsion angles) are used to interpret the: Φ (phi), Ψ (psi) and ω (omega), indicating rotation about each of three repeating bonds in peptide backbone.

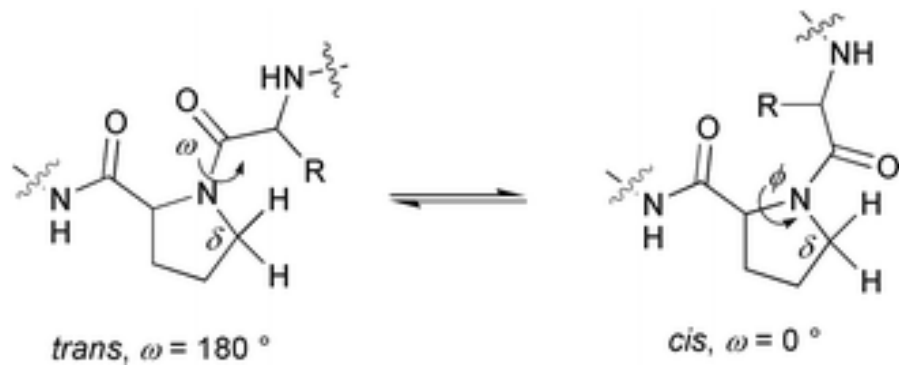


Figure 1.1: Trans and cis conformation of peptide bonds

Because of the partial double-bond character of peptide bond between C and N, the rotation around it is restricted. There are only two conformations which the atoms

$\text{C}\alpha$, O, C, N, $\text{C}\alpha_{+1}$ are all in one plane are energetically preferred: when dihedral angle $\omega = \pm 180^\circ$, the peptide bond is in trans configuration, while $\omega = 0^\circ$, peptide bond is in cis configuration (Figure 1.1).

In the majority of cases, peptide bond is found to be trans configuration (99.6% of the time)³. The rationale behind this preponderance of trans peptide bond is believed to lie in the energy difference between trans and cis forms. Because of the steric repulsion between neighboring side chains, the cis form is less stable. Early in 1960s, researchers found there is a high energy barrier (~ 20 kcal/mol) of the trans-cis isomerization, which leads cis-trans isomerization as a rate-limiting step in protein folding (Figure 1.2).⁵ Due to the cis-trans isomerization, cis-peptide bond may compromise the homogeneity of protein and hinder the crystallization study of protein.

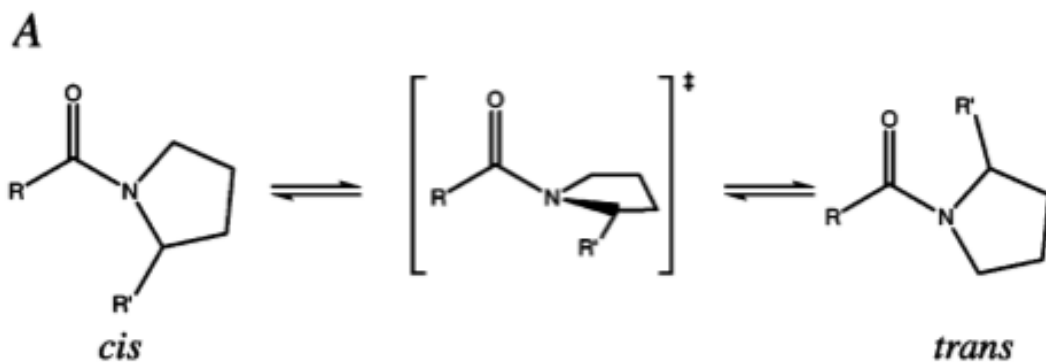


Figure 1.2: Cis-trans isomerization of a prolyl peptide bond. A transition state is involved in this one-step mechanism.

Though trans peptide bond have a predominant advantage, cis peptide bond is still essential for the protein structure maintain. Most of cis peptide bond is found in β conformation due to its amenable form for a tight turn.³ The presence of a cis peptide bond in β conformation give peptide chain great flexibility to change direction.

Steinbrecher et al found that β turn of type IV contains around 26% of all cis peptide bond.⁷

There are two kinds of cis peptide bond: Xaa-Pro (Xaa represents any amino acids) and Xaa-nonPro peptide bond. Proline cis-peptide bond is found to be much favorable during the study of cis peptide bond. Weiss et al found about there are about 5.21% Xaa-Pro cis peptide bond but only 0.028% Xaa-nonPro in protein (include resolution structure $<2.0 \text{ \AA}$, $2.0 \text{ \AA} - 2.5 \text{ \AA}$ and $\geq 2.5 \text{ \AA}$) via a set of 571 proteins from PDB bank. They also pointed out that high resolution structure ($<2.0 \text{ \AA}$) contains twice of Xaa-Pro cis peptide bond and four times of Xaa-nonPro cis peptide bond in medium resolution structure ($2.0 \text{ \AA} - 2.5 \text{ \AA}$). The existence of cis-peptide bond is possibly not that rare as we used to believe. Therefore, the resolution of protein structure is an important factor for the detection of cis peptide bond.⁸

The prevalence of proline in cis peptide bond is because proline experience similar steric clashes in both the cis and trans conformation due to its rigid sidechain. Study found there is a smaller entropy loss in the conversion from trans to cis in prolyl peptide groups than in non-prolyl peptide groups.⁹ Moreover, compared to the prolyl cis-peptide bond, the cis-trans isomerization of non-prolyl cis-peptide bond has an additional cost of $\sim 2 \text{ kcal/mol}$ (based on the energy barrier $\sim 20 \text{ kcal/mol}$).

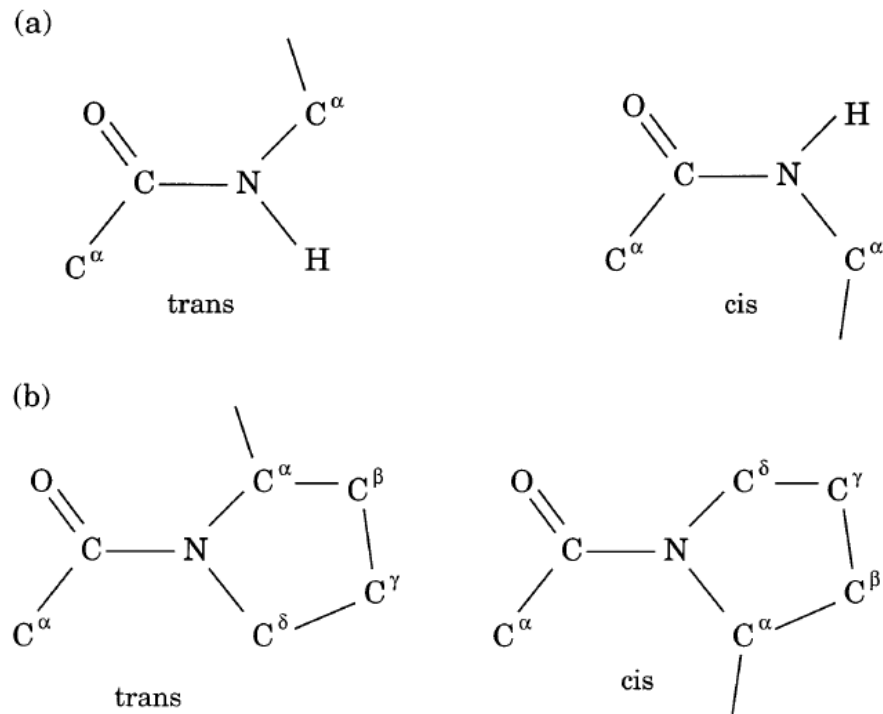


Figure 1.3: Non-proline (a) and proline (b) peptide fragments in trans and cis conformations.

Despite of the high energy barrier of cis-trans isomerization, the existence of cis peptide bond in protein is essential for both structural and functional reasons. For example, cis peptide bond can play a role on the enzyme activity. A non-Pro cis peptide bond was reported in the structure of Chitinase B, located at Glu-144 and Tyr-145 in active site at the center of the TIM barrel.¹¹ Study also shows it involved in direct contact with substrate while it also stays close to the interface of dimer.¹² (Figure 1.4 A) The prolyl cis peptide bond in Glycinamide ribonucleotide synthetase enzymes was found next to the active site of synthetase, which is believed to affect the

formation of glycinamide ribonucleotide.¹³ Beside the influence on the enzyme activity, cis peptide bond was also found to be part into the protein interaction. A prolyl cis-peptide bond was observed to directly take part in the interaction between the N-terminal Zn²⁺ ribbon domain and the cystathionine beta synthase domain in a novel protein from *Thermoplasma acidophilum* (Figure 1.4 B).¹⁴

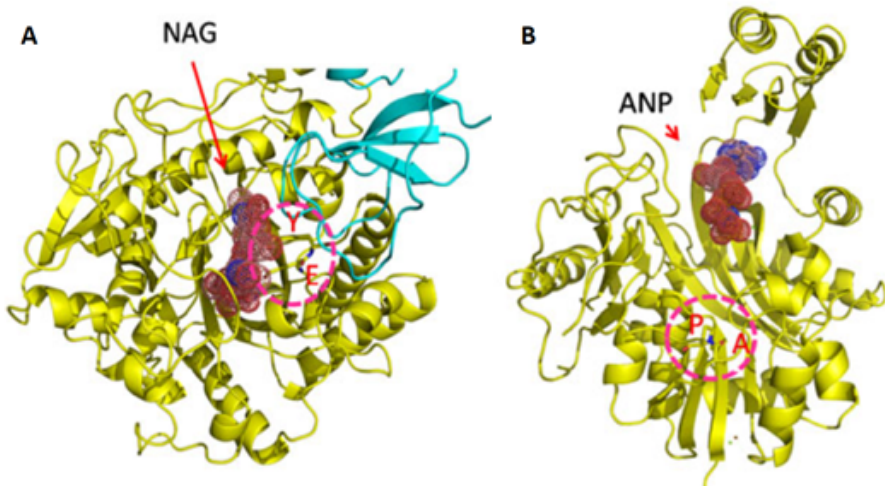


Figure 1.4: Function of cis peptide bond in protein. **(A)** The structure of Chitinase B (PDB ID: 1GOI) (yellow) highlighting the binding site of N-acetyl D-glucosamine (NAG) (orange). The residues involved in cis peptide (EY) are also indicated (red). The other monomer is shown in cyan. **(B)** The structure of glycinamide ribonucleotide synthetase from *E. coli* (yellow) that holds a cis peptide (AP) at the active site. The ADP-binding site is also highlighted, ANP phosphoaminophosphonic acid adenylate ester

1.2 Platelet-Activating Factor Acetylhydrolase (PAF-AH)

Platelet-activating factor acetylhydrolase (PAF-AH), also known as lipoprotein-associated phospholipase A2 (Lp-PLA₂), is a group VIIA PLA₂ enzyme that catalyzes the hydrolysis of platelet- activating factor (PAF).¹⁵ PAF (1-O-alkyl-2-acetyl-sn-glycero-3-phosphocholine), as a pro-inflammatory mediator, displays a diverse spectrum of biological effect. PAF-AHs can catalyze the hydrolysis of acetyl group at the sn-2 position of PAF, with yield of lyso-PAF and acetate (Figure 1.5). Besides PAF, there are also a wide range of substrate that can be hydrolyzed by PAF-AH, such as oxidized phospholipids from LDL oxidation. Unlike other PLA₂ protein, PAF-AH can only hydrolyze substrates with short acetyl chain at sn-2 position.¹⁷ In order to ensure the cellular function integrity, PAF-AHs cannot hydrolyze normal cellular phospholipids during they present in an active form inside or outside the cells.

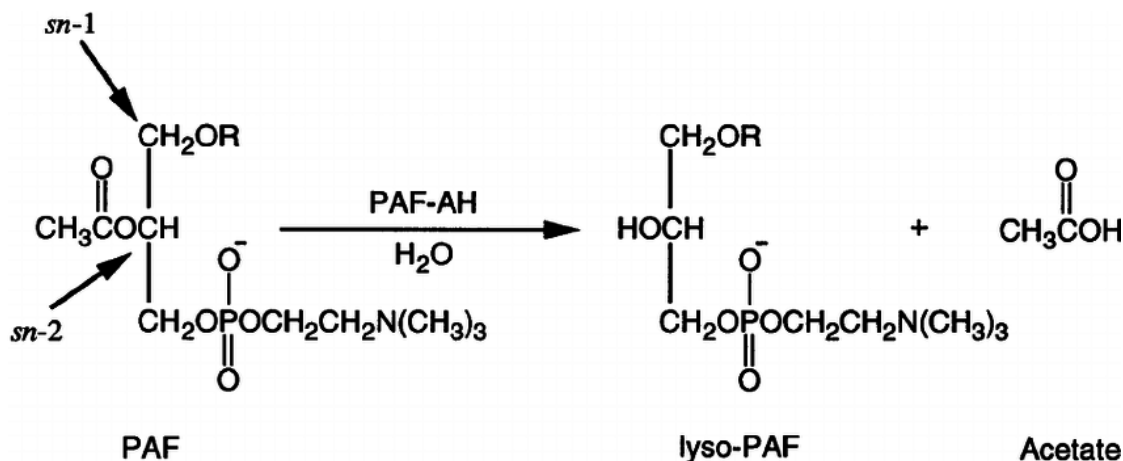


Figure 1.5: PAF-AH catalyzes the hydrolysis of PAF to lyso-PAF and acetate.

There are three different types of PAF-AH that have been reported: plasma PAF-AH, PAF-AH Ib and PAF-AH II.¹⁹ As part of the Ca⁺ independent neutral lipases

and serine esterase, three of them all contain the highly conserved GXSXG or GXSXV motif. The intracellular PAF-AH Ib is mostly found in the brain and contains two catalytic α subunits (two α subunits share 63% sequence identity) and one β subunits. According to its solved structure through x-ray crystallography, there was reported to have no homology or identity with other two PAF-AHs.²⁰

PAF-AH II is an intracellular N-myristoylated enzyme and located in the cytoplasma of liver and kidney cells. It responds to oxidative stress by becoming increasingly bound to endoplasmic reticulum and Golgi membranes. It was reported to be a necessary enzyme for protecting cells from oxidative stress induced apoptosis.²⁹ Unlike PAF-AH Ib, PAF-AH II was reported to share 41% sequence identity with Plasma PAF-AH.^{21, 22}

Plasma PAF-AH is an extracellular monomer, circulates in plasma and associates with lipoproteins. The structure of Plasma PAF-AH has been solved via x-ray crystallography (Figure 1.6).²³ As confirmed by the solved crystal structure, plasma PAF-AH contains a classic lipase α/β -hydrolase fold with a Ser, Asp and His catalytic triad. The serine is located at the conserved GXSXG motif. According the crystal structure, there is also a rare, non-prolyl cis-peptide bond in Lp-PLA₂ between residues Phe72 and Asp73. Research shows that a majority of PAF-AH is associated with low density lipoprotein (LDL) and a small portion with high density lipoprotein (HDL).²⁴

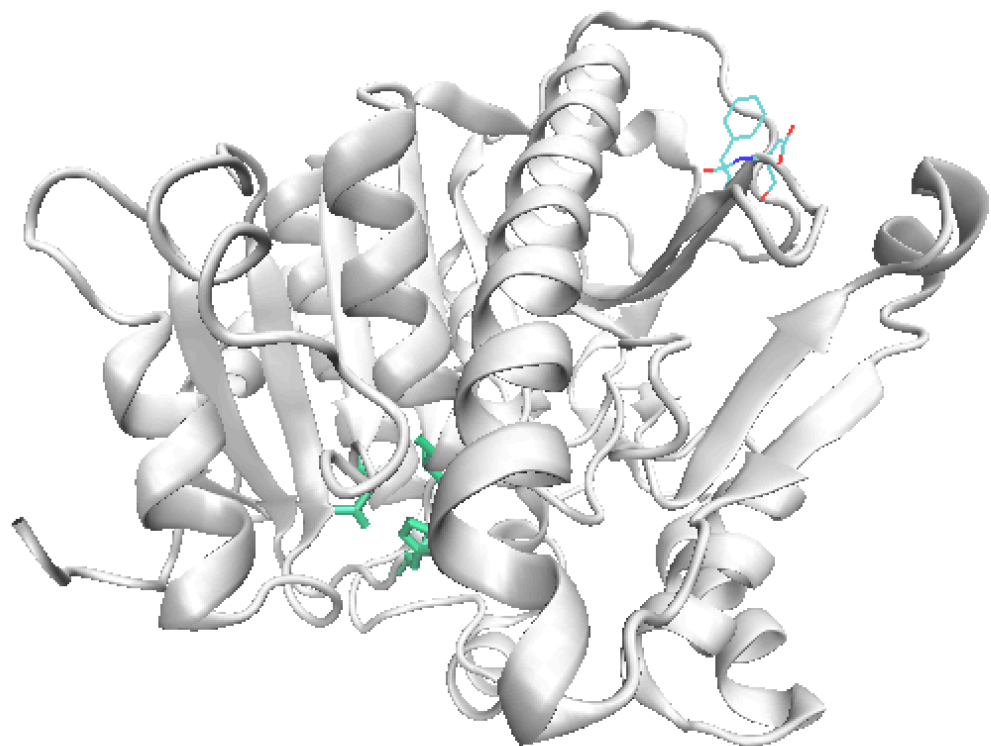


Figure 1.6: Structure of plasma PAF-AH. Cartoon view is the whole structure plasma PAF-AH. The catalytic triad Ser-273, Asp-296 and His-351 are shown in green sticks. The position of non-prolyl cis-peptide bond at Phe-72 and Asp-73 is shown in blue lines.

Plasma PAF-AH has been obtained high attention from scientists for the past several years since the first discovery of the link between the increase of Plasma PAF-AH concentration or activity to an increased risk of cardiovascular diseases(CVD).²⁵ It is well known that the initiation and progress of CVD is greatly associated with the severity of atherosclerosis, which is acknowledged as a chronic and dynamic status of vascular inflammation. Currently, plasma PAF-AH is recognized as a pro-inflammatory enzyme which plays a role in regulation of lipid metabolism and inflammatory respond. A widely accepted hypothesis is proposed that PAF-AH might lead to the vascular inflammation during atherosclerosis because of its ability to form pro-inflammatory substance.²⁶ Based on this acknowledgement, a large number of studies pointed out that PAF-AH could be used as a biomarker to assess the risk of coronary heart diseases (CHD). In the light of this hypothesis, researchers proposed that the inhibition of PAF-AH activity could decrease the risk of vascular atherogenesis, which leads to many reversible PAF-AH inhibitors were developed in pharmaceutical industry. However, there are some controversies about the dual pro-inflammatory or anti-inflammatory effect of plasma PAF-AH on atherosclerosis. The reason why plasma PAF-AH is regarded as anti-inflammatory is its ability to hydrolyze PAF and oxidized lipoproteins, both of which are known as harmful to vessel wall.³⁰ Some research found that the increase of PAF-AH concentration could alleviate vascular inflammation and attenuate atherosclerosis in various animal models. However, on the contrary, the decrease of PAF-AH due to the mistake mutation could cause the greatly increasing risk of cardiovascular (CV).^{31, 32} Though the role of plasma PAF-AH in atherosclerosis is still obscured, currently a widely accepted view

is that plasma PAF-AH associated with LDL is pro-atherosclerotic while plasma PAF-AH associated with HDL is anti-atherosclerotic.²⁷

However, despite the high attention on plasma PAF-AH, there are still a lot of unsolved question about plasma PAF-AH. The mechanism behind the LDL and HDL binding is still obscure. The function of such a rare non-prolyl cis-peptide bond in plasma PAF-AH remains unsolved. Therefore, based on the former research of Lp-PLA₂ and solved crystal structure, a hypothesis for the function of this non-prolyl cis peptide bond is going to described below.

1.3 Non-Prolyl Cis Peptide Bond in Plasma PAF-AH

As the description above in section 1.1, non-prolyl cis peptide bond is scarce in protein due to the high activation energy barrier from cis-trans isomerization. Therefore, they usually play a vital role in the proteins such as help maintain the function of the protein and control the protein auto-inhibition. Moreover, the cis-trans isomerization can also involve in the ion channel gating control.²⁸

Plasma PAF-AH has a non-prolyl cis peptide bond between Phe-72 and Asp-73 (Figure 1.7). This cis-peptide bond is part of β -hairpin extending from Ser-64 to Ser-87. As the solved crystal structure shows, the cis peptide bond is far away from the catalytic triad. Therefore, it might have little chance to affect the enzyme activity.

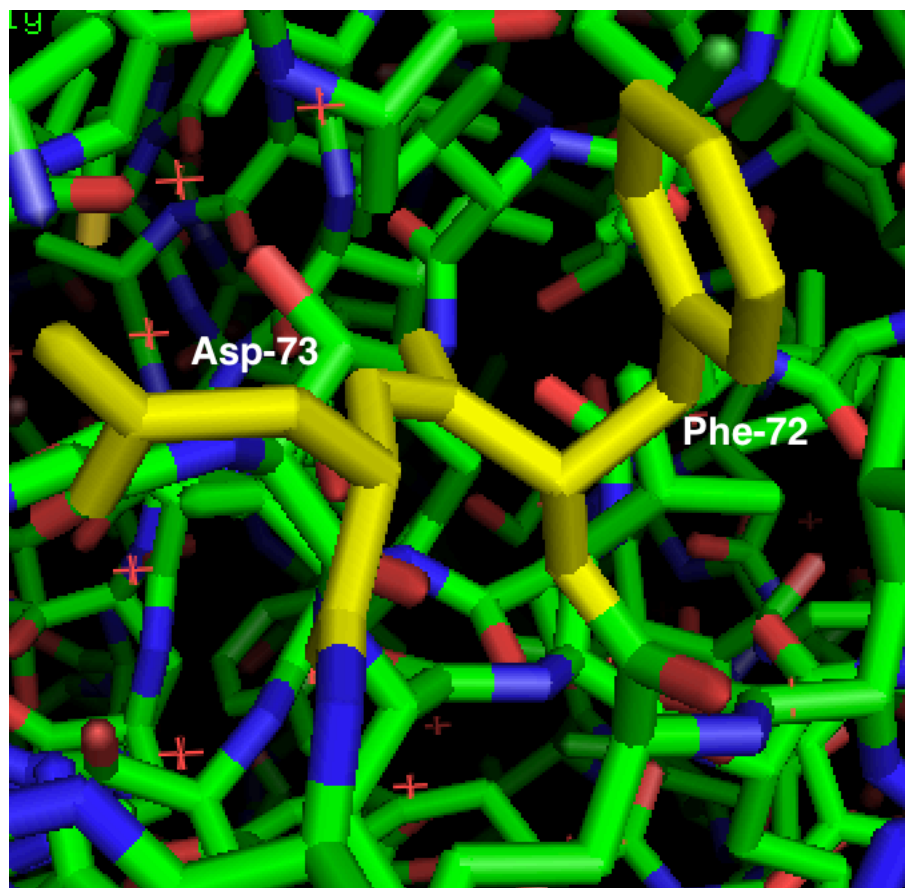


Figure 1.7: Stick diagram of Phe-72 and Asp-73 in plasma PAF-AH, shown in yellow.

Most of the plasma PAF-AH in Humans is binding to LDL and HDL.

Researches show that the majority of Humans plasma PAF-AH is bound to LDL while only a small portion is bound to HDL. Though the mechanism behind the interaction with two lipoproteins is still obscure, the common understanding is that distinct regions of plasma PAF-AH interact with LDL and HDL particles. Helix 363-369 in C

terminal consists of the binding site for HDL particles and helix 114-125 in N terminal is for LDL particles.

The reason why plasma PAF-AH shows to have a higher affinity to LDL binding is unclear, but the apoB, as the apolipoprotein only present in LDL but not in HDL, are shown to mediate the interaction between the plasma PAF-AH and LDL particles.

Moreover, the crystal structure of PAF-AH shows that there is a stretch of negatively charged amino acids, an acidic patch, which possibly plays a role in the interaction with apoB (Figure 4). As Figure 4 shows, Y205 residue is very close to the acidic patch, consistent with the reckoning presented above.

Aromatic amino acids are known for the stabilization ability of π interaction. Considering the cation-pi interaction between K109 and Y205 (Figure 1.8A), the apoB's clusters of positively charged residues and the acidic patch region, there could be a possibility that the Phe cis-peptide bond could mediate the interaction between the Y205 and apoB. Thereby the interaction between plasma PAF-AH and LDL could be stabilized.

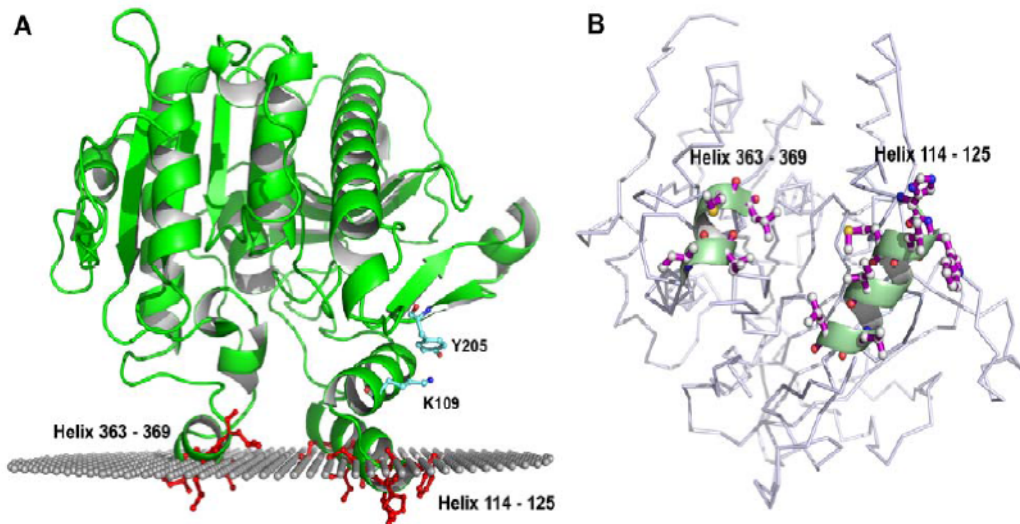


Figure 1.8: Orientation of PAF-AH on a membrane surface, predicted by OPM. **(A)** i-face residue for lipoprotein binding are showing in red. K109 and Y205 are found to display a cation-π interaction, showing in blue. **(B)** The i-face residues are shown after a ~90° rocation of view from (A)

Table 1.1 Amino acids predicted for lipoprotein binding in plasma PAF-AH

i-face amino acids	Charged amino acids	
	Basic patch	Acidic Patch
Helix 114-125: H114, W115, L116, M117, I120, L123, L124	K55, R58, K363, K101, R122, H367, K370	D374, D376, D382, D401, D403, D406, D412, D413, E414
Helix 363-369: I364, I365, M368, L369		

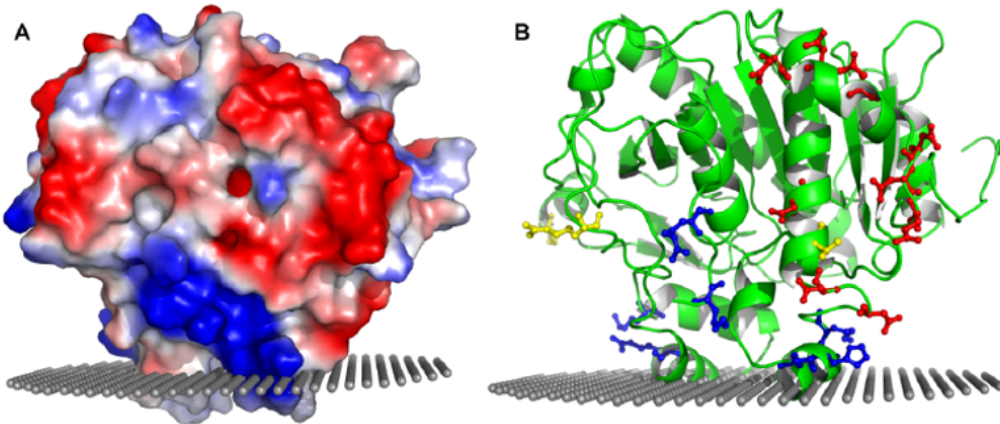


Figure 1.9: Acidic and basic patches. **(A)**The surface electrostatic potential view of PAF-AH, acidic patches showing in red, basic patches showing in blue. **(B)** Amino acids in acidic patches are showing in red while amino acids in basic patches are showing in blue.

Moreover, researches show that majority of plasma PAF-AH in mouse is bound to HDL. According to the sequencing alignment results of plasma PAF-AH from different mammals, residue-73 in mouse plasma PAF-AH is glycine. Though the structure of mouse plasma PAF-AH is unsolved, there is a great chance that the peptide bond between Phe-72 and Gly-73 of mouse plasma PAF-AH is in trans configuration based on the hypothesis described above.

Figure 1.10: Sequencing alignment result of plasma PAF-AH from mammals.

In order to prove the authenticity of the hypothesis, two mutations were produced at the site of this non-prolyl cis-peptide bond. The first one is D73G, involved the mutagenesis of Asp-73 to glycine, which is aimed to mimic the peptide bond between 72rd and 73th residue in mouse plasma PAF-AH. The second one is D73P, involved the mutagenesis of Asp-73 to proline, which is aimed to change the non-prolyl cis-peptide bond to more favorable prolyl cis-peptide bond to explore the rationale behind that.

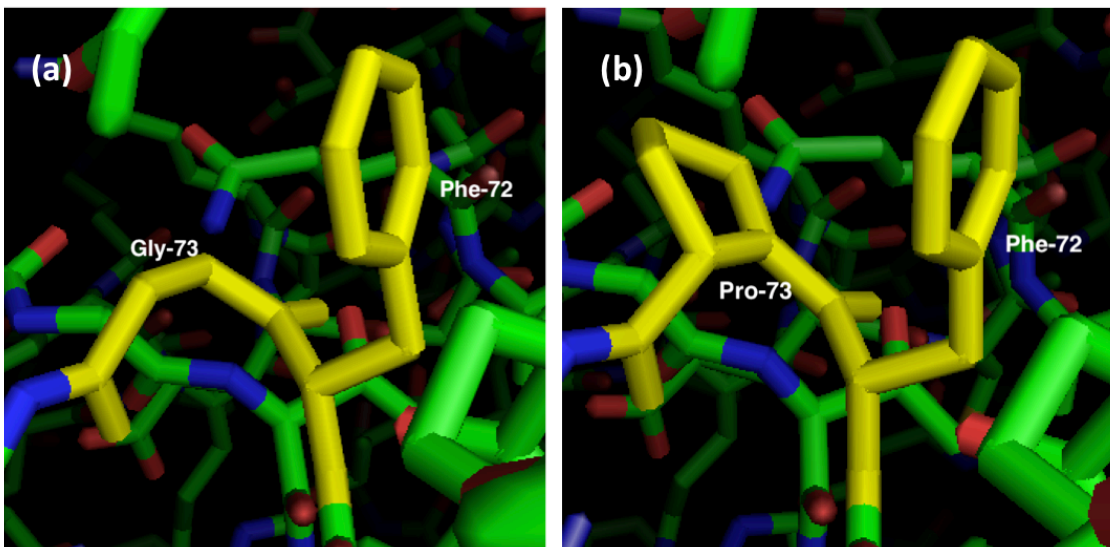


Figure 1.11 Stick diagram of Mutagenesis in PAF-AH featuring location 72 and 73.
(a) Featuring Phe-72 and Gly-73, shown in yellow; (b) Featuring Phe-72 and Pro-73, shown in yellow.

REFERENCES

1. Donald Voet, Judith G. Voet, Charlotte W. Pratt. Fundamentals of Biochemistry, 4th ed.; Ch.6.
2. Maison, Wolfgang, et al. "Multicomponent synthesis of tripeptides containing pipecolic acid derivatives: selective induction of cis-and trans-imide bonds into peptide backbones." *Journal of the Chemical Society, Perkin Transactions 1* 12 (2000): 1867-1871.
3. Nelson, David L., Albert L. Lehninger, and Michael M. Cox. *Lehninger principles of biochemistry*. Macmillan, 2008.
4. Craveur, P., Joseph, A. P., Poulain, P., de Brevern, A. G., Rebehmed, J. (2013) Cis-Trans Isomerization of Omega Dihedrals in Proteins. *Amino Acids*. 45, 279-289.
5. Steinberg, Izchak Z., et al. "The configurational changes of poly-L-proline in solution." *Journal of the American Chemical Society* 82.20 (1960): 5263-5279.
6. Andreotti, Amy H. "Native state proline isomerization: an intrinsic molecular switch." *Biochemistry* 42.32 (2003): 9515-9524.

7. Stewart, David E., Atom Sarkar, and John E. Wampler. "Occurrence and role of cis peptide bonds in protein structures." *Journal of molecular biology* 214.1 (1990): 253-260.
8. Weiss, Manfred S., Andreas Jabs, and Rolf Hilgenfeld. "Peptide bonds revisited." *Nature Structural & Molecular Biology* 5.8 (1998): 676-676.
9. Zimmerman, S. Scott, and Harold A. Scheraga. "Stability of cis, trans, and nonplanar peptide groups." *Macromolecules* 9.3 (1976): 408-416.
10. Wedemeyer, William J., Ervin Welker, and Harold A. Scheraga. "Proline cis-trans isomerization and protein folding." *Biochemistry* 41.50 (2002): 14637-14644.
11. Kolstad, G., B. Synstad, and V. G. H. Eijsink. "Structure of the D140N mutant of chitinase B from *Serratia marcescens* at 1.45 Å resolution." *Acta Crystallographica Section D: Biological Crystallography* 58.2 (2002): 377-379.
12. van Aalten, Daan MF, et al. "Structural insights into the catalytic mechanism of a family 18 exo-chitinase." *Proceedings of the National Academy of Sciences* 98.16 (2001): 8979-8984.
13. Wang, Weiru, et al. "X-ray crystal structure of glycinamide ribonucleotide synthetase from *Escherichia coli*." *Biochemistry* 37.45 (1998): 15647-15662.

14. Proudfoot, Michael, et al. "Biochemical and structural characterization of a novel family of cystathionine β -synthase domain proteins fused to a Zn ribbon-like domain." *Journal of molecular biology* 375.1 (2008): 301-315.
15. Blank, Merle L., et al. "A specific acetylhydrolase for 1-alkyl-2-acetyl-sn-glycero-3-phosphocholine (a hypotensive and platelet-activating lipid)." *Journal of Biological Chemistry* 256.1 (1981): 175-178.
16. Honda, Zen-ichiro, Satoshi Ishii, and Takao Shimizu. "Platelet-activating factor receptor." *The Journal of Biochemistry* 131.6 (2002): 773-779.
17. Steinbrecher, Urs P., and P. Haydn Pritchard. "Hydrolysis of phosphatidylcholine during LDL oxidation is mediated by platelet-activating factor acetylhydrolase." *Journal of lipid research* 30.3 (1989): 305-315.
18. Soubeyrand, Sebastien, and Puttaswamy Manjunath. "Platelet - activating factor acetylhydrolase in seminal plasma: A brief review." *Molecular reproduction and development* 50.4 (1998): 510-519.
19. Six, David A., and Edward A. Dennis. "The expanding superfamily of phospholipase A 2 enzymes: classification and characterization." *Biochimica et Biophysica Acta (BBA)-Molecular and Cell Biology of Lipids* 1488.1 (2000): 1-19.

20. Hattori, Mitsuharu, et al. "Miller-Dieker lissencephaly gene encodes a subunit of brain platelet-activating factor." *Nature* 370.6486 (1994): 216-218.
21. Matsuzawa, Atsushi, et al. "Protection against oxidative stress-induced cell death by intracellular platelet-activating factor-acetylhydrolase II." *Journal of Biological Chemistry* 272.51 (1997): 32315-32320.
22. Hattori, Kenji, et al. "Purification and characterization of platelet-activating factor acetylhydrolase II from bovine liver cytosol." *Journal of Biological Chemistry* 270.38 (1995): 22308-22313.
23. Samanta, Uttamkumar, and Brian J. Bahnsen. "Crystal structure of human plasma platelet-activating factor acetylhydrolase structural implication to lipoprotein binding and catalysis." *Journal of Biological Chemistry* 283.46 (2008): 31617-31624.
24. Stafforini, D. M., et al. "Human plasma platelet-activating factor acetylhydrolase. Association with lipoprotein particles and role in the degradation of platelet-activating factor." *Journal of Biological Chemistry* 262.9 (1987): 4215-4222.

25. Sudhir, Krishnankutty. "Lipoprotein-associated phospholipase A2, a novel inflammatory biomarker and independent risk predictor for cardiovascular disease." *The Journal of Clinical Endocrinology & Metabolism* 90.5 (2005): 3100-3105.
26. MACPHEE, Colin H., et al. "Lipoprotein-associated phospholipase A2, platelet-activating factor acetylhydrolase, generates two bioactive products during the oxidation of low-density lipoprotein: use of a novel inhibitor." *Biochemical Journal* 338.2 (1999): 479-487.
27. Wilensky, Robert L., and Colin H. Macphee. "Lipoprotein-associated phospholipase A2 and atherosclerosis." *Current opinion in lipidology* 20.5 (2009): 415-420.
28. Lu, Kun Ping et al. "Prolyl Cis-Trans Isomerization As A Molecular Timer". *Nature Chemical Biology* 3.10 (2007): 619-629. Web.
29. Inoue, Takao, et al. "Type II platelet-activating factor-acetylhydrolase is essential for epithelial morphogenesis in *Caenorhabditis elegans*." *Proceedings of the National Academy of Sciences of the United States of America* 101.36 (2004): 13233-13238.

30. Macphee, Colin H. "Lipoprotein-associated phospholipase A 2: a potential new risk factor for coronary artery disease and a therapeutic target." *Current opinion in pharmacology* 1.2 (2001): 121-125.
31. Turunen, Päivi, et al. "Adenovirus-mediated gene transfer of Lp-PLA2 reduces LDL degradation and foam cell formation in vitro." *Journal of lipid research* 45.9 (2004): 1633-1639.
32. Jang, Yangsoo, et al. "Carriage of the V279F null allele within the gene encoding Lp-PLA2 is protective from coronary artery disease in South Korean males." *PloS one* 6.4 (2011): e18208.

Chapter 2

MOLECULAR CLONING AND MUTAGENESIS OF ΔPAF-AH

2.1 Introduction

Plasma ΔPAF-AH is mainly secreted by macrophages during their differentiation from monocytes. It was first discovered in the early 1980s due to its ability to hydrolase the pro-inflammatory glycerophospholipid PAF. In 1986, human plasma PAF-AH was first purified from human plasma by Stafforini and co-workers.² In order to separate the PAF-AH with LDL, various of detergents were tested and they finally found Tween 20 could well resolve the LDL protein.² In 1995, by screening a monocyte-derived macrophages cDNA library via polymerase chain reaction (PCR), the human plasma PAF-AH gene was first cloned by Tjoelker et al. According to the report, Plasma PAF-AH is encoded by PLA2G7 gene with 12 exons and composes of 441 amino acids.³

Plasma PAF-AH is 441 amino acids in length. In order to get a better result of crystallization screening, a truncated human plasma PAF-AH construct (ΔPAF-AH) of residue 49-423 was produced by Dr. Prabhavathi Srinivasan from the Bahnsen lab. The construct lacks 18 amino acids at C-terminus to increase the solubility of protein. It also eliminates 8 non-native amino acids at N-terminus which are believed to hinder the crystallization. All truncated parts are known to be unnecessary for the protein folding and enzyme activity.⁴ Molecular cloning for this work would be carried out by

the recombinant Δ PAF-AH, which was cloned into a bacterial expression vector, pGEX-6P1. The mutant constructs of plasma PAF-AH were generated by site-directed mutagenesis.

2.2 Materials and Methods

2.2.1 Materials

The pGEX-6P-1 vector was from the lab the Dr. Catherine Grimes. Δ PAF-AH, in the vector of pGEX-6P-1, was obtained from Kaitlyn Worner from the Bahnsen lab. The PCR primers and carbenicillin were from Sigma-Aldrich. The Luria-Bertani media(LB) and agarose were from Fisher Scientific. The dNTP mix was purchased from Promega. The QIAquick PCR Purification Kit was from Qiagen.

2.2.2 Molecular cloning of Δ PAF-AH

Δ PAF-AH in the vector of pGEX-6P-1 was PCR amplified by using 1 μ L ds DNA template (30 ng/ μ L), 2 μ L forward primer, 2 μ L reverse primer, 5 μ L dNTP mix, 25 μ L DNA polymerase. The PCR procedure was performed using the following primers and PCR parameter:

Forward primer (BamHI site underlined)

5'- AAAAAAAGGATCCTCCTTGGCCAAACT - 3'

Reverse primer (SalI site underlined)

5'- AAAAAACAGCTGGTTAATGTTGGTCCCCT - 3'

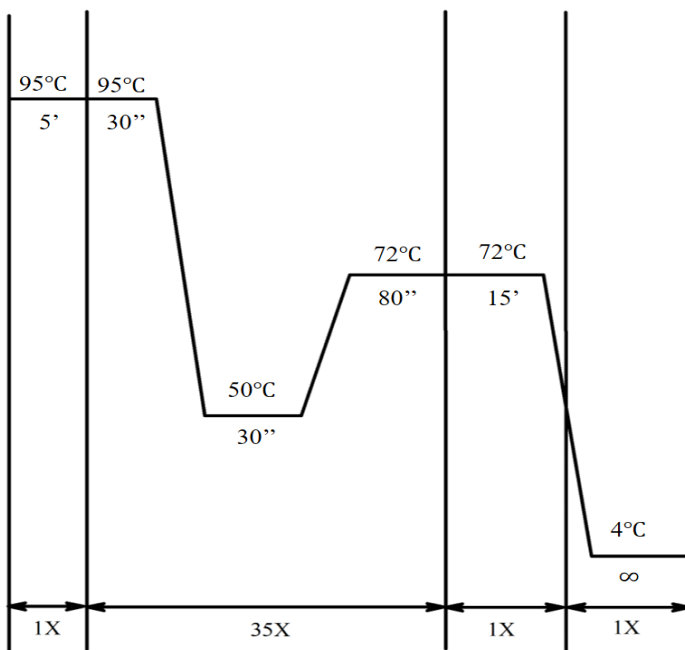


Figure 2.1: The PCR parameter for the amplification of Δ PAF-AH in pGEX-6P1 vector.

The PCR product was digested with DPN1 and transformed into BL21 chemically competent cells. Cells from individual single-colonies were grown in 5 mL culture overnight. Then, a glycerol stock of construct in BL21 cells was made and stored at -80 °C, while cells from overnight culture were purified by using QIAquick PCR Purification Kit and sent to GENEWIZ (South Plainfield, NJ) for DNA sequencing.

2.2.3 Mutagenesis of Δ PAF-AH

2.2.3.1 D73P

Via the site directed mutagenesis, the 73rd residue was mutated from aspartate to proline. The PCR procedure was performed by using 1 μ L plasmid DNA (30 ng/ μ L), 2.5 μ L forward primer, 2.5 μ L reverse primer, 5 μ L dNTP mix, 25 μ L DNA polymerase. The mutation of Asp-73 was performed using the following primers and PCR parameter:

Forward primer (mutation site underlined)

5'- GTACAGACTTAATGTTTCCTCACACTAATAAGGGCACC - 3'

Reverse primer

5'- GGTGCCCTTATTAGTGTGAGGAAACATTAAGTCTGTAC - 3'

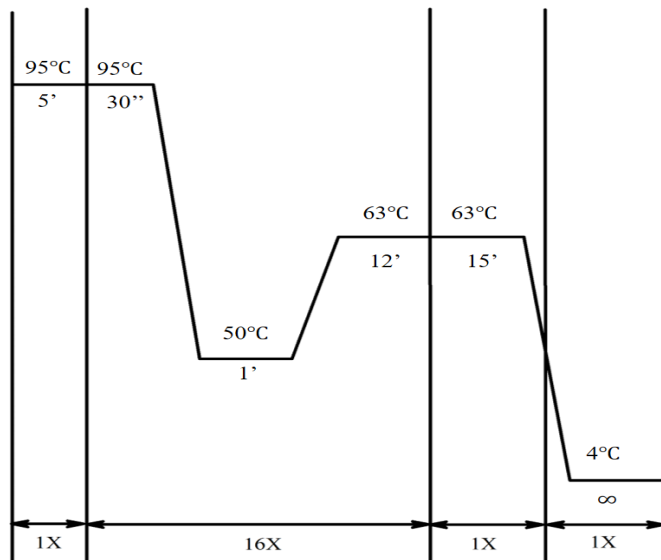


Figure 2.2: The PCR parameter for the mutation of 73rd residues of Δ PAF-AH in pGEX-6P1 vector from aspartate to proline.

The melting temperature of D73P mutagenesis primer set is 64 °C, the annealing temperatures of this gradient were chosen to be lower than the T_m .

In order to confirm the mutagenesis was successful, a 0.8% agarose gel was run. Then the PCR product was digested with DPN1 and transformed into DH5 α and BL21 chemically competent cells through electrocompetent transformation. Cells from individual single-colonies were grown overnight in 5 mL cultures. Then, a glycerol stock of construct in cells was made and stored at -80 °C, while cells from overnight culture were purified by using QIAquick PCR Purification Kit and sent out for DNA sequencing (GENEWIZ, South Plainfield, NJ).

2.2.3.2 D73G

The mutagenesis of 73rd residue from aspartate to glycine was performed as same as the 2.2.3.1 did. Via the site directed mutagenesis, the PCR procedure was performed by using 1 μ L plasmid DNA (30 ng/ μ L), 2 μ L forward primer, 2 μ L reverse primer, 5 μ L dNTP mix, 25 μ L DNA polymerase. The mutation of Asp-73 was performed using the following primers and PCR parameter:

Forward primer (mutation site underlined)

5'- CAGACTTAATGTTGGTACACTAATAAGGGC - 3'

Reverse primer

5'- GCCCTTATTAGTGACCAACATTAAGTCTG - 3'

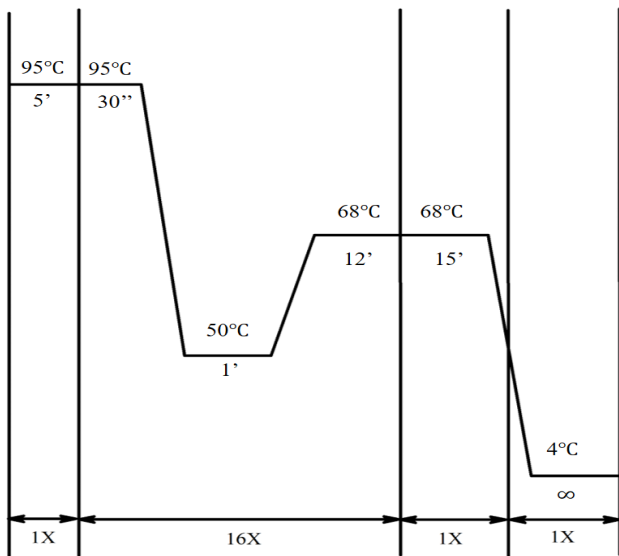


Figure 2.3: The PCR parameter for the mutation of 73rd residues of Δ PAF-AH in pGEX-6P1 vector from aspartate to glycine.

The melting temperature of D73G mutagenesis primer set is 69.7 °C and the annealing temperatures of this gradient were chosen to be lower than the T_m .

A 0.8% agarose gel was run to confirm the success of mutagenesis. After the digestion with DPN1, the mutagenesis product was transformed into DH5 α and BL21 chemically competent cells via electrocompetent transformation. Cells from individual single-colonies were grown overnight in 5 mL culture. Then, a glycerol stock of construct in cells was made and stored at -80 °C, while cells from overnight culture were purified by using QIAquick PCR Purification Kit and sent out for DNA sequencing (GENEWIZ, South Plainfield, NJ).

2.3 Results and Discussion

The PCR production of wild type ΔPAF-AH, mutant construct D73P and D73G was confirm via DNA sequencing. A sequence alignment was accomplished by using those DNA sequencing results. The alignment was performed via Culstal Omega software (Figure 2.4). The site directed mutations were performed quiet successful.

WT	GGCCAAACTAAAATCCCCGGGGAAATGGGCCTTATTCCGTTGGTTGTACAGACTTAATG
D73G	GGCCAAACTAAAATCCCCGGGGAAATGGGCCTTATTCCGTTGGTTGTACAGACTTAATG
D73P	GGCCAAACTAAAATCCCCGGGGAAATGGGCCTTATTCCGTTGGTTGTACAGACTTAATG

WT	TTTGATCACACTAATAAGGGCACCTTCTTGC GTTTATATTATCCATCCAAGATAATGAT
D73G	TTTGGTCACACTAATAAGGGCACCTTCTTGC GTTTATATTATCCATCCAAGATAATGAT
D73P	TTTCCTCACACTAATAAGGGCACCTTCTTGC GTTTATATTATCCATCCAAGATAATGAT
***	*****
WT	CGCCTTGACACCCTTGGATTCCAATAAGAATATT TTGGGTCTTAGCAAATTCTT
D73G	CGCCTTGACACCCTTGGATTCCAATAAGAATATT TTGGGTCTTAGCAAATTCTT
D73P	CGCCTTGACACCCTTGGATTCCAATAAGAATATT TTGGGTCTTAGCAAATTCTT

WT	GGAACACACTGGCTTATGGCAACATTTGAGGTTACTCTTGGTTCAATGACAACCTCCT
D73G	GGAACACACTGGCTTATGGCAACATTTGAGGTTACTCTTGGTTCAATGACAACCTCCT
D73P	GGAACACACTGGCTTATGGCAACATTTGAGGTTACTCTTGGTTCAATGACAACCTCCT

WT	GCAAAC T GGAATTCCCTCTGAGGCCTGGT GAAAAAATCCACTTGTGTTCTCAT
D73G	GCAAAC T GGAATTCCCTCTGAGGCCTGGT GAAAAAATCCACTTGTGTTCTCAT
D73P	GCAAAC T GGAATTCCCTCTGAGGCCTGGT GAAAAAATCCACTTGTGTTCTCAT

WT	GGTCTTGGGCATT CAGGACACTTATTCTGCTATTGGCATTGACCTGGCATCTCATGGG
D73G	GGTCTTGGGCATT CAGGACACTTATTCTGCTATTGGCATTGACCTGGCATCTCATGGG
D73P	GGTCTTGGGCATT CAGGACACTTATTCTGCTATTGGCATTGACCTGGCATCTCATGGG

Figure 2.4: Sequencing alignment results for ΔPAF-AH and cis-peptide bond mutants D73G and D73P

2.4 Conclusions

In this chapter, the molecular cloning and mutagenesis of the plasma platelet-activating factor acetylhydrolase (PAF-AH) was presented. Two site-directed mutants-D73G and D73P were made. The DNA sequencing result alignment shows the accomplishment of mutagenesis and set the first step for the following study.

REFERENCES

1. Elstad, M. R., et al. "Platelet-activating factor acetylhydrolase increases during macrophage differentiation. A novel mechanism that regulates accumulation of platelet-activating factor." *Journal of Biological Chemistry* 264.15 (1989): 8467-8470.
2. Stafforini, D. M., Stephen M. Prescott, and Thomas M. McIntyre. "Human plasma platelet-activating factor acetylhydrolase. Purification and properties." *Journal of Biological Chemistry* 262.9 (1987): 4223-4230.
3. Tjoelker, Larry W., et al. "Anti-inflammatory properties of a platelet-activating factor acetylhydrolase." *Nature* 374.6522 (1995): 549.
4. Tjoelker, Larry W., et al. "Plasma platelet-activating factor acetylhydrolase is a secreted phospholipase A2 with a catalytic triad." *Journal of Biological Chemistry* 270.43 (1995): 25481-25487.

Chapter 3

EXPRESSION AND PURIFICATION OF PAF-AH

3.1 Introduction

The purification and expression of recombinant plasma PAF-AH in *E. coli* was standardized in laboratory by Tjoelker et al.^{1,2} ΔPAF-AH and cis-peptide bond mutants were expressed in chemical competent cells BL21 and induced by IPTG.³ All constructs were first purified by a glutathione sepharose column and incubated with PreScission Protease to cleave the GST tag. In order to get high-purity protein samples for continuing characterization and crystallization trial, cleaved protein samples were applied to the FPLC for further purification.

For the optimization of protein purification, the pH of system buffer was dependent on the isoelectric point (pI) of ΔPAF-AH and all cis-peptide bond mutants. The pI of each construct was calculated via ExPASy Compute pI tool. The result is showing at Table3.1. Therefore, a buffer system at pH 7.8 was used for purification of wild type ΔPAF-AH and a buffer system at pH 8.1 was for D73G and D73P mutants to ensure a net negative charge of protein.

Table 3.1 Predicted pI for Δ PAF-AH and cis-peptide bond mutants

PAF-AH Construct	Predicted pI	pH of system buffer
Δ PAF-AH	6.68	7.8
D73G	6.95	8.1
D73P	6.95	8.1

3.2 Materials and Methods

3.2.1 Materials

Ampicillin, ATP, MgCl₂, 4-nitrophenylacetate (PNPA), Triton X-100 and lysozyme were from Sigma-Aldrich. TrisBase, Tris hydrochloride, NaCl, pepstatin, dithiothreitol (DTT), TEMED, reduced glutathione, bis-Acrylamide, molecularporous membrane tubing, SDS, Ethylenediaminetetraacetic acid (EDTA) and sodium acetate were from Fisher Scientific. Ammonium persulfate was purchased from Promega. Acrylamide and 2-(N-morpholino) ethanesulfonic acid (MES) was from Acros. The glutathione sepharose 4 fast flow and HiTrap Q HP column (5 mL) was from GE Healthcare Life Sciences. Isopropyl β -D-1-thiogalactopyranoside was purchased from Goldbio.com. All other materials for the expression and purification of PAF-AH are listed in Chapter 2.

3.2.2 Expression of ΔPAF-AH and mutants in E.coli

A little scrape of the glycerol stock was grown shaking overnight in 200 mL of Luria-Bertani (LB) media with 100 µg/mL ampicillin at 30 °C as a starter culture. In the following morning 10 mL of overnight culture was grown shaking in 1 L of fresh LB media with 100 µg/mL ampicillin at 30 °C until it's OD₆₀₀ ≈ 0.8 (about 4 h). The culture was induced with 1.0 mM IPTG and left shaking overnight at 18 °C. The cells were collected by centrifugation at 8,000 rpm (Sorvall SLA-3000) for 8 min at 4 °C. Pelleted cells were stored at -80 °C for later purification.

3.2.3 Purification of ΔPAF-AH and mutants

The purification of PAF-AH was developed based on the research of previous lab member Kaitlyn Worner.

3.2.3.1 Protein affinity chromatography

Pelleted cells were thawed at cold room (~4 °C) for about 1 h and resuspended in 50 mM Tris buffer containing 100 mM NaCl, 1 mM DTT, 1 µM pepstatin and 0.1 mg/mL lysozyme at pH 7.8 or pH 8.1 depending on the construct being purified. Cells were lysed by sonication three times of 2 min each with 3 min rest between. Then lysed cells were rocked at 4 °C with 0.1% Triton X-100 for 30 min to solubilize PAF-AH fusion and isolate from the cell membrane. Then the suspension was centrifuged at 12,000 rpm (Sorvall SS-34) at 4 °C for 20 min. Then the supernatant was incubated with 10 mM ATP and 20 mM MgCl₂ for 15 min at 4 °C to remove the chaperone from fusion protein. Then a second centrifugation at 12,000 rpm at 4 °C for 20 min was performed. During the second centrifugation the columns with glutathione sepharose resin were equilibrated with 2 column wash buffer containing 50 mM Tris base, 100

mM NaCl, 1 mM DTT, 5 mM ATP, 20 mM MgCl₂ and 0.1% Triton X-100 at pH 7.8 or pH 8.1. Supernatant was applied to the equilibrated column and rocked for incubation at 4 °C for at least 1h to ensure fusion protein was bound to the resin. After the incubation, the column was drained and washed by 300 mL equilibration buffer. Then 300 ml wash buffer containing 50 mM Tris base, 100 mM NaCl, 1 mM EDTA, 1 mM DTT and 0.1% Triton X-100 at pH 7.8 or pH 8.1 was applied to the column. About 8 mL of wash buffer was left in the column with 800 µL PreScission Protease for incubation overnight at 4 °C to cleave the GST-tag from the fusion protein. In the following morning, cleaved protein was collected and stored at 4 °C for later use. To remove the PreScission Protease and GST-tag, two column of wash buffer containing 0.1 M tris hydrochloride, 0.5 M NaCl at pH 8.5 was applied, then followed by two-column of 0.1 M sodium acetate and 0.5 M NaCl wash buffer at pH 4.5. Then the column was stored at 4 °C with 20% alcohol.

Considering the strong band at GST-tag position on SDS page for cleaved protein, a second incubation in glutathione sepharose column was applied to cleaved protein. A small column (~10 mL) with Glutathione sepharose resin was equilibrated with two-column of 50 mM tris and 100 mM NaCl wash buffer at pH 7.8 or pH 8.1. After equilibration, cleaved protein was applied to the column and rocked at 4°C for 1h to further remove the GST-tag. The interested protein was collected and store at 4 °C for further purification. To remove the GST-tag on the resin, same procedure was applied to the small column as mentioned above.

3.2.3.2 Q-sepharose anion exchange chromatography

Cleaved protein sample was dialyzed overnight into 2 L of running buffer containing 50 mM Tris, 1 mM EDTA, 20 mM NaCl, 1 mM DTT and 0.005% Triton X-100 at pH 7.8 or pH 8.1. After overnight dialysis the cleaved protein was concentrated by Amicon Ultra centrifugal filter units (30 kDa molecular weight cut-off, Millipore) at 2000 rpm (Sorvall SH-3000) to a final volume less than 1 mL. A Q-sepharose anion exchange FPLC column (5 mL) was equilibrated by 15 mL water, followed by low salt buffer containing 50 mM Tris, 1 mM EDTA, 20 mM NaCl, 1 mM DTT and 0.005% Triton X-100 at pH 7.8 or pH 8.1 at a 1.0 mL/min flow rate. Then the concentrated protein sample was loaded onto the FPLC and bound to Q-sepharose resin. Then the resin was wash by low salt buffer with 20 mL at 1.0 mL/min flow rate to remove any nonspecific binding. A linear gradient elution buffer was then performed with high salt buffer containing 50 mM Tris, 1 mM EDTA, 750 mM NaCl, 1 mM DTT and 0.005% Triton X-100 at pH 7.8 or pH 8.1 over 75 mL, ranging from 0% - 100% at the same flow rate. Then over 20 mL high salt wash buffer was applied to Q-sepharose column to remove remaining bound protein. During the gradient elution, fractions were collected as the spikes in UV graph were shown, usually the pure protein began to elute between 300 and 350 mM NaCl. Fractions containing pure protein were collected together and store at 4 °C for further characterization.

3.2.3.3 Size-exclusion chromatography

Cleaved protein sample was dialyzed overnight into 2 L of running buffer containing 50 mM Tris, 1 mM EDTA and 150 mM NaCl at pH 7.8 or pH 8.1. After overnight dialysis, the cleaved protein was concentrated by Amicon Ultra centrifugal filter units (30 kDa molecular weight cut-off, Millipore) at 2000 rpm (Sorvall SH-3000) to a final volume less than 1 mL. A size-exclusion FPLC column (25 mL) was equilibrated by 50 mL water, followed by 25 mL of wash buffer containing 50 mM Tris, 1 mM EDTA, 150 mM NaCl, at pH 7.8 or pH 8.1 at a 0.75 mL/min flow rate. Then the concentrated protein sample was loaded onto the FPLC and bound to size-exclusion resin. An hour-long elution buffer was run with the same wash buffer. Then over 50 mL water was applied to size-exclusion column to remove remaining bound protein at 0.75 mL/min flow rate. During the elution, fractions were collected as the spikes in UV graph were shown. Fractions containing pure protein were collected together and store at 4 °C for further characterization.

3.2.4 Purification of PreScission Protease

Pelleted cells with recombinant PreScission Protease stored at -80 °C were thawed at 4 °C for 1h. Then cells were re-suspended in lysis buffer containing 50 mM Tris, 150 mM NaCl and 2 mM DTT at pH 8.0. Cells were lysed by sonication three times of 2 min each with 3 min rest between. Then the suspension were centrifuged at 14,000 rpm (Sorvall SS-34) at 4 °C for 15 min twice to ensure the clarity of soluble supernatant. During the second centrifugation the columns with glutathione sepharose resin were equilibrated with 3 column volumes of wash buffer containing 50 mM Tris, 150 mM NaCl and 2 mM DTT at pH 8.0. Supernatant was applied to the equilibrated

column and rocked for incubation at 4 °C for 2 h to ensure fusion protein was bound to the resin. After the incubation, the flow through was discarded. The column was washed with wash buffer until the OD 280 was less than 0.075. The elution was performed by using 2 mL fraction of 50 mM Tris, 150 mM NaCl and 2 mM DTT and 10 mM GSH (add fresh) at pH 8. It took about 40 mL before the OD 280 was less than 0.075. The elution was run on an SDS page gel to ensure the purity. The protein sample was dialyzed overnight into 4 L of 50 mM Tris, 150 mM NaCl and 2 mM DTT at pH 8.0 to remove the GSH. Then 86% glycerol was added to dilute protein 2-fold. 0.8 mL aliquots were stored at -80 °C until use.

3.2.5 BCA Assay

In order to determine the concentration of pure protein, BCA protein assay (Pierce) was performed to protein sample. Work curve was made by using bovine serum albumin (BSA) standards, ranging from 0.125 mg/mL to 2 mg/mL. 50 parts of BCA reagent A was mixed with 1 part of BCA reagent B to form working reagent. Then BSA standards and protein samples were incubated with 1mL of working reagent each at 37 °C for 30 min. Then the samples were applied to UV machine and read the absorbance at 562 nm. A working curve was made by BSA standards absorbance to determine the concentration of protein samples.

3.2.6 PNPA activity assay

Para-nitrophenyl acetate (PNPA), as a common serine esterase substrate, is usually used to assess serine hydrolase activity. Its structure and chemistry mechanism

are shown below. Formation of para-nitrophenoxide ion can be monitored by an increase in absorbance at 405 nm. This assay was carried out in 1 mL volumes of 50 mM Tris buffer, pH 7.5 with 5 mM PNPA at room temperature. The assay was initiated with the addition of 1 μ L purified Δ PAF-AH or mutants (protein concentration was ranging from 1-4 mg/mL). The change in absorbance at 405 nm was measured for 30 s and the activity of purified protein was determined. In order to accurately calculate the enzyme specific activity, the molar coefficient of para-nitrophenoxide was determined by preparing a calibration curve using known concentration of para-nitrophenoxide ranging from 0.01 mM to 0.1 mM. (Molar extinction coefficient was $\epsilon=13950\text{ M}^{-1}\cdot\text{cm}^{-1}$)

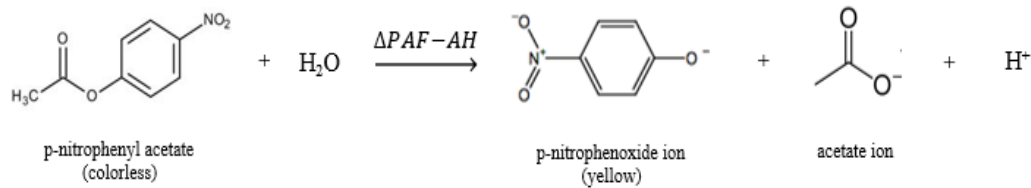


Figure 3.1 PAF-AH hydrolyze PNPA to p-nitrophenoxide and acetate.

3.3 Results and Discussion

3.3.1 Expression and purification of ΔPAF-AH and mutants

ΔPAF-AH and two cis-peptide bond mutants were expressed in *E. coli* (BL21 chemically competent cells). ΔPAF-AH, D73G and D73P were expressed simultaneously in *E. coli* about 4 h, and induced with 1 mM IPTG overnight for the growth of desired proteins. In order to ensure the desired protein was well expressed during cells culture, SDS-PAGE test was performed on whole cells obtained before and after overnight induction with IPTG to visualized the relative quantities of fusion protein. Cells samples were collected and diluted to a proper concentration for SDS PAGE. Then diluted samples were lysed with SDS PAGE sample buffer. The SDS PAGE was shown that ΔPAF-AH, D73G and D73P mutant constructs were expressed well during overnight induction. It could be seen by the presence of a strong band at the position of fusion proteins (69 kDa) in three lanes of induced whole cells when compared to the lanes of uninduced whole cells. From these results, it can be ensured that the substitution of Asp-73 for proline residues and glycine residues did not change the production of fusion proteins during expression.

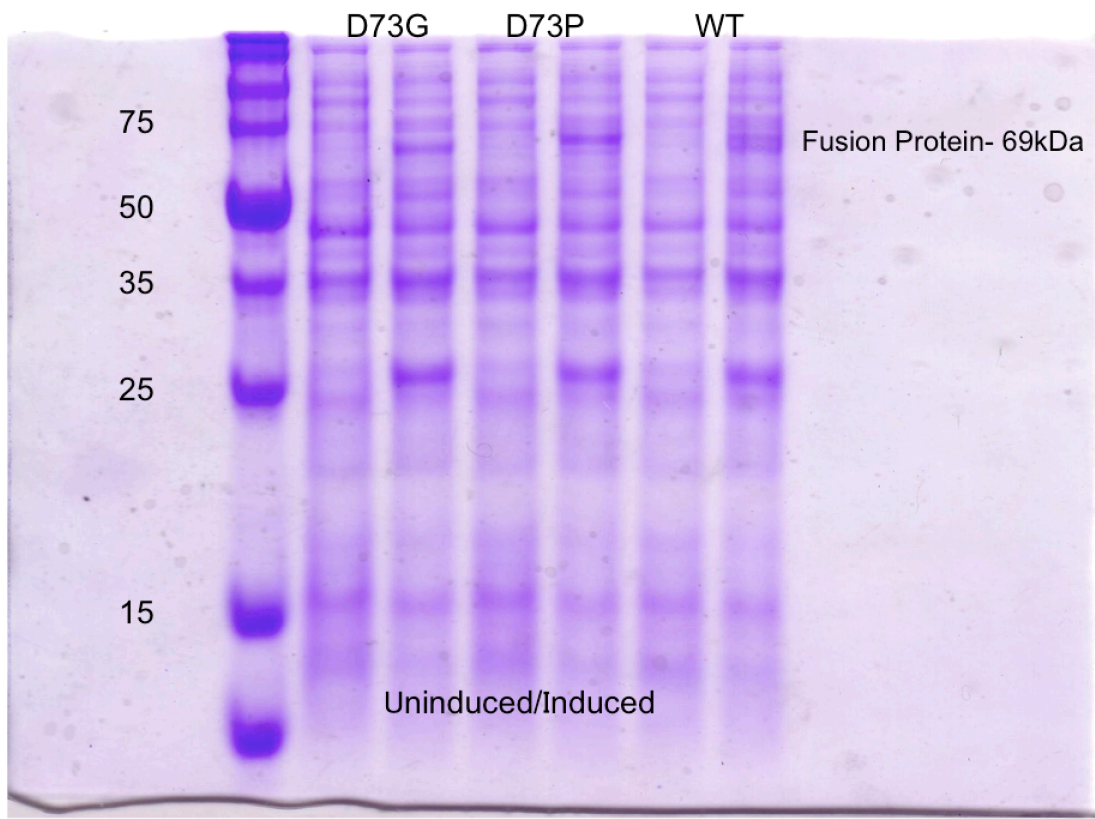


Figure 3.2: SDS PAGE for the cells expression of D73G, D73P and Δ PAF-AH before and after overnight induction with 1 mM IPTG.

In the light of its predicted pI of 6.68, Δ PAF-AH fusion proteins were purified in pH 7.8 buffering system. Δ PAF-AH was first purified via a Glutathione Sepharose column, with yielding of 1.78 mg of recombinant protein per liter of cell culture. The yield of all purified Δ PAF-AH and mutant constructs was determined via BCA assay.

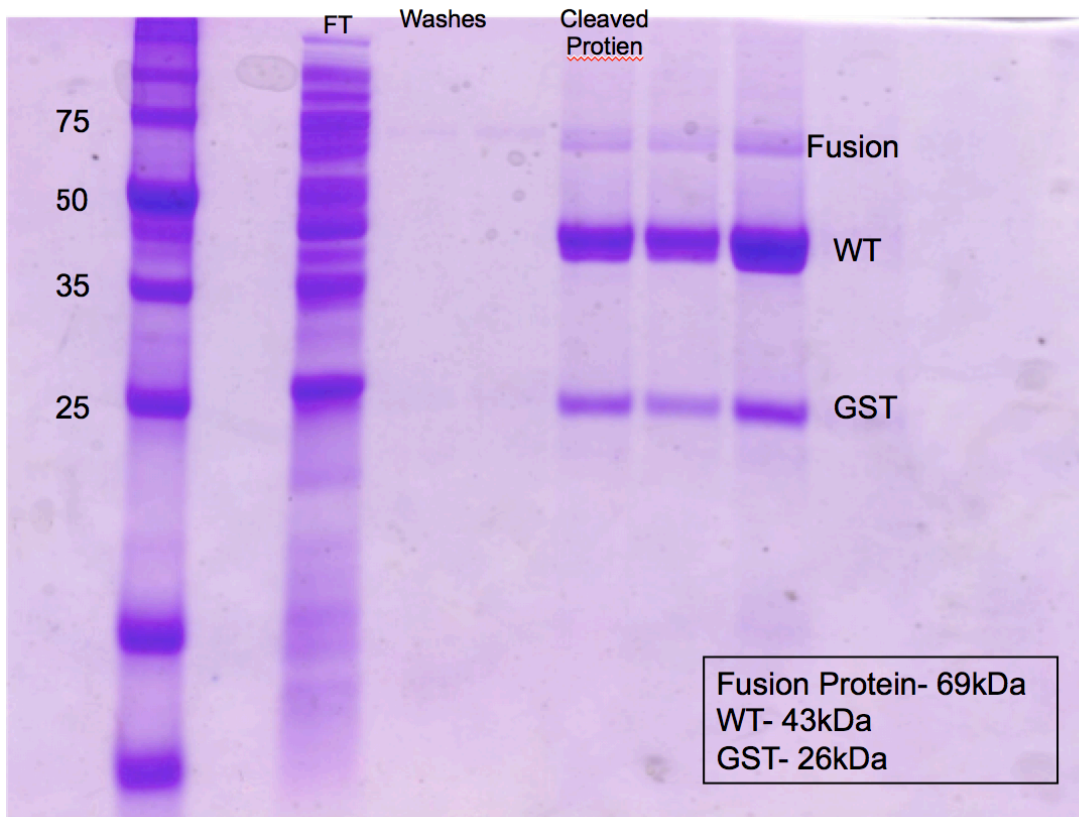


Figure 3.3: SDS PAGE for wild type Δ PAF-AH after purification via a glutathione sepharose column. The yield is 1.78 mg protein per liter of cell culture, with the purity ~83.5%

The purity of the purified protein of SDS PAGE sample was determined by using ImageJ software and was quantified to be approximately 83.5%. Due to this purity was not enough for the crystallization trial, size exclusion chromatography was performed to further increase the purity of the protein sample. After size exclusion chromatography, the purity of protein sample was found to be approximately 97.5%, with a reduced yielding of 1.32 mg of fusion protein per liter of cell culture. Protein

might have been lost during the protein concentration process (protein samples would precipitate because of high concentration) and the protein-loading process in size exclusion chromatography. The protein sample was collect and stored at 4 °C for further characterization.

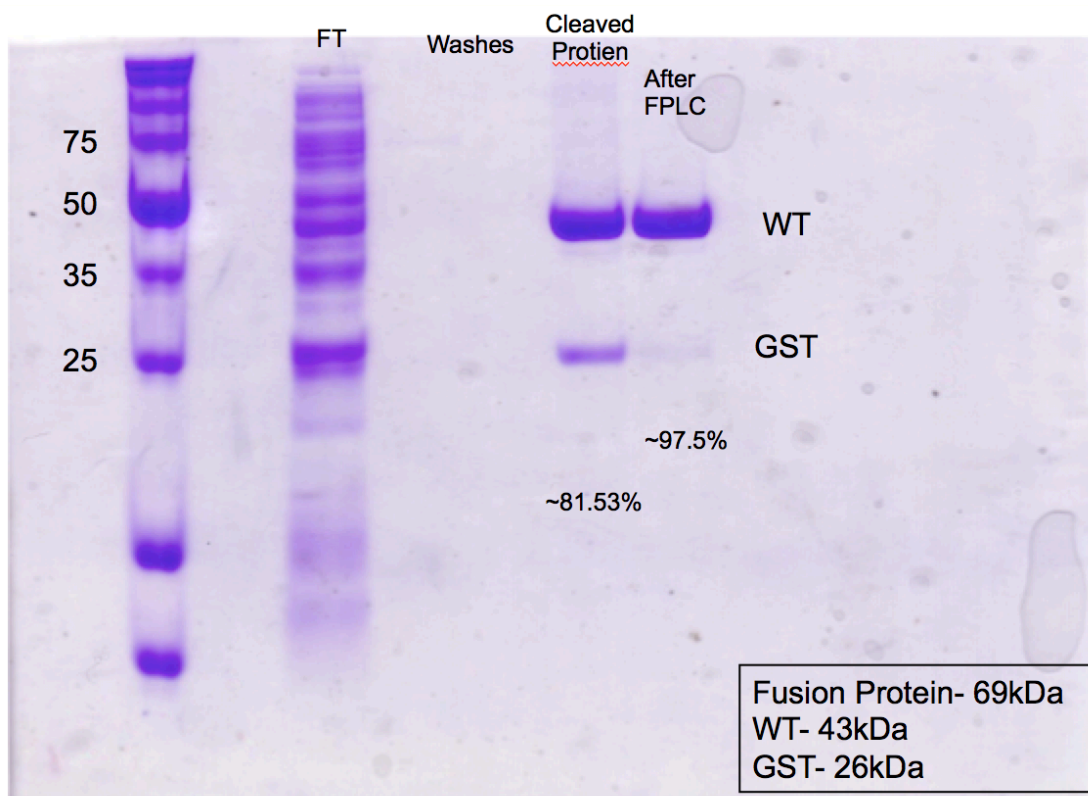


Figure 3.4: SDS PAGE for wild type ΔPAF-AH after second purification via size exclusion chromatography. The yield is 1.32 mg protein per liter of cell culture, with the purity ~97.5%

D73G and D73P mutant constructs were purified in pH 8.1 buffering system in the light of their predicted pI of 6.95. D73G was purified via a Glutathione Sepharose column, with yielding of 1.57 mg of recombinant protein per liter of cell culture.

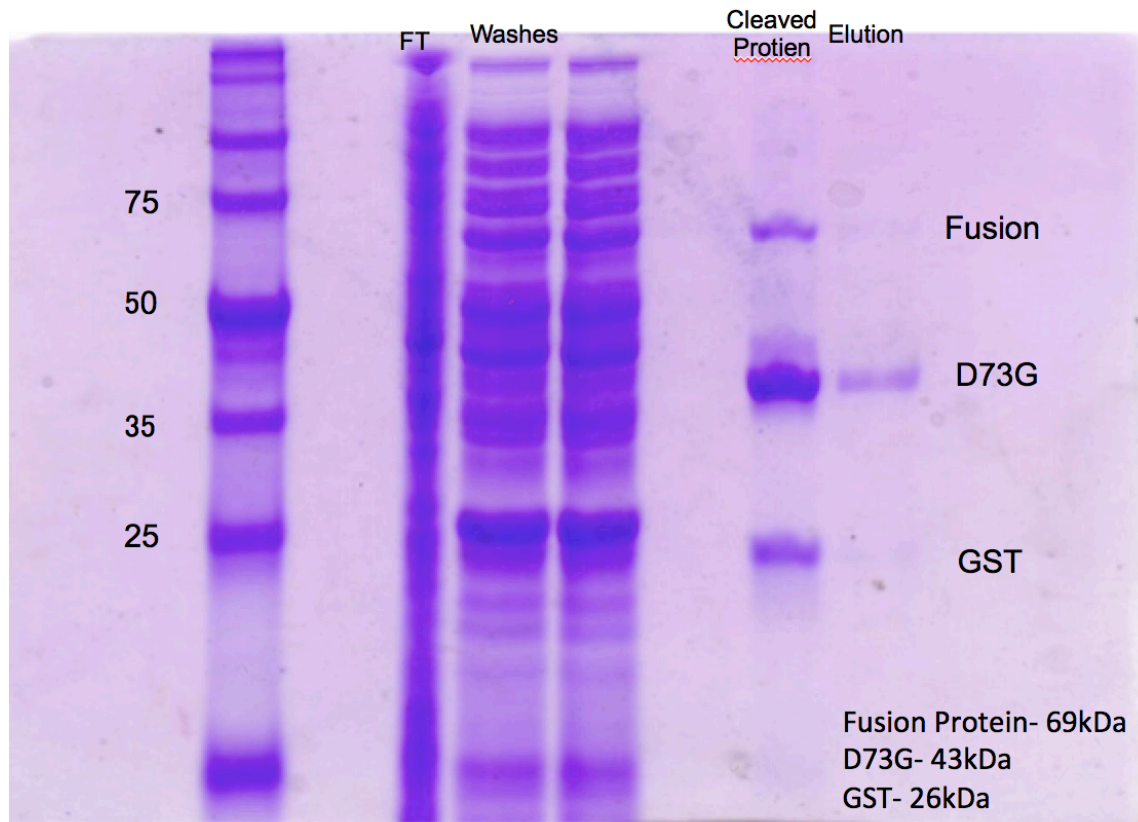


Figure 3.5: SDS PAGE for cis-peptide bond mutant D73G after purification via a glutathione sepharose column. The yield is 1.57 mg protein per liter of cell culture, with the purity ~78.6%

The purity of the purified protein of SDS PAGE sample was determined by using ImageJ software and was quantified to be approximately 78.6%. Due to this purity was not enough for the crystallization trial, Q-sepharose anion exchange chromatography was performed to further increase the purity of the protein sample. After size exclusion chromatography, the purity of protein sample was found to be approximately 93.1%, with a final yielding of 1.14 mg of fusion protein per liter of cell culture. The protein sample was collect and stored at 4 °C for further characterization.

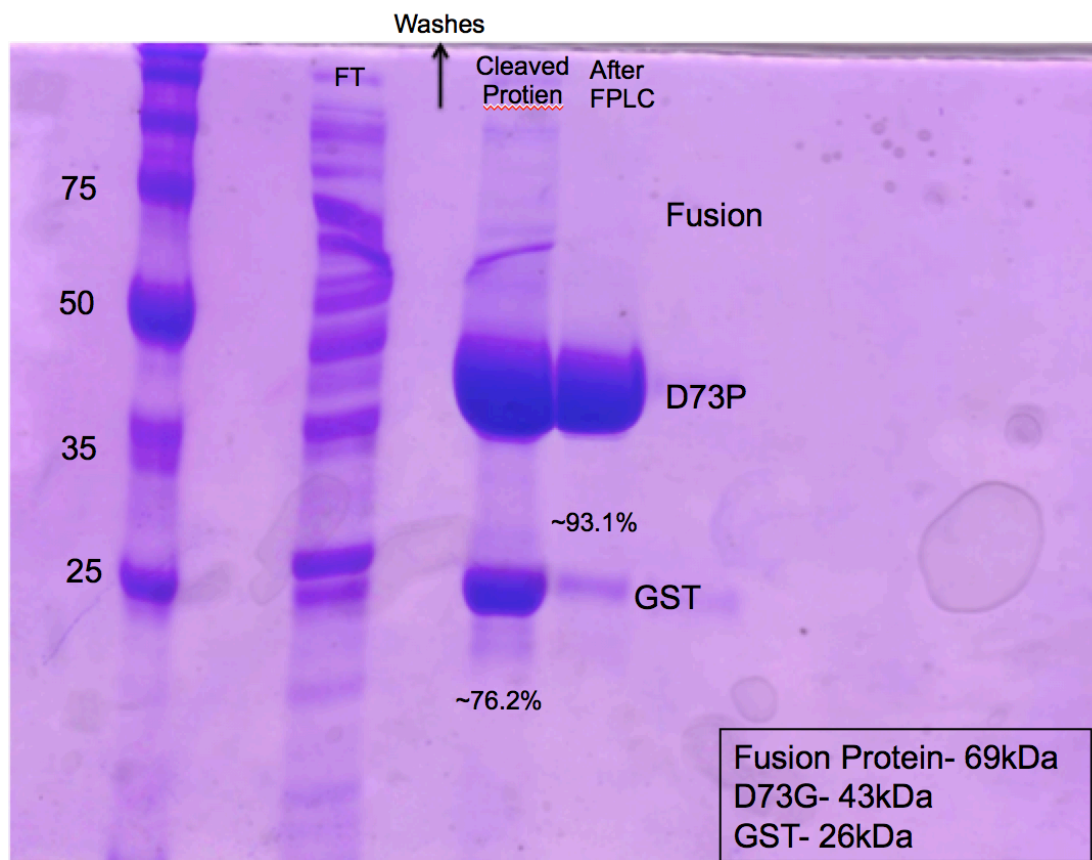


Figure 3.6: SDS PAGE for cis-peptide bond mutant D73G after second purification via Q-sepharose anion exchange chromatography. The yield is 1.14 mg protein per liter of cell culture, with the purity ~93.1%

D73P was purified via a Glutathione Sepharose column, with yielding of 1.65 mg of recombinant protein per liter of cell culture.

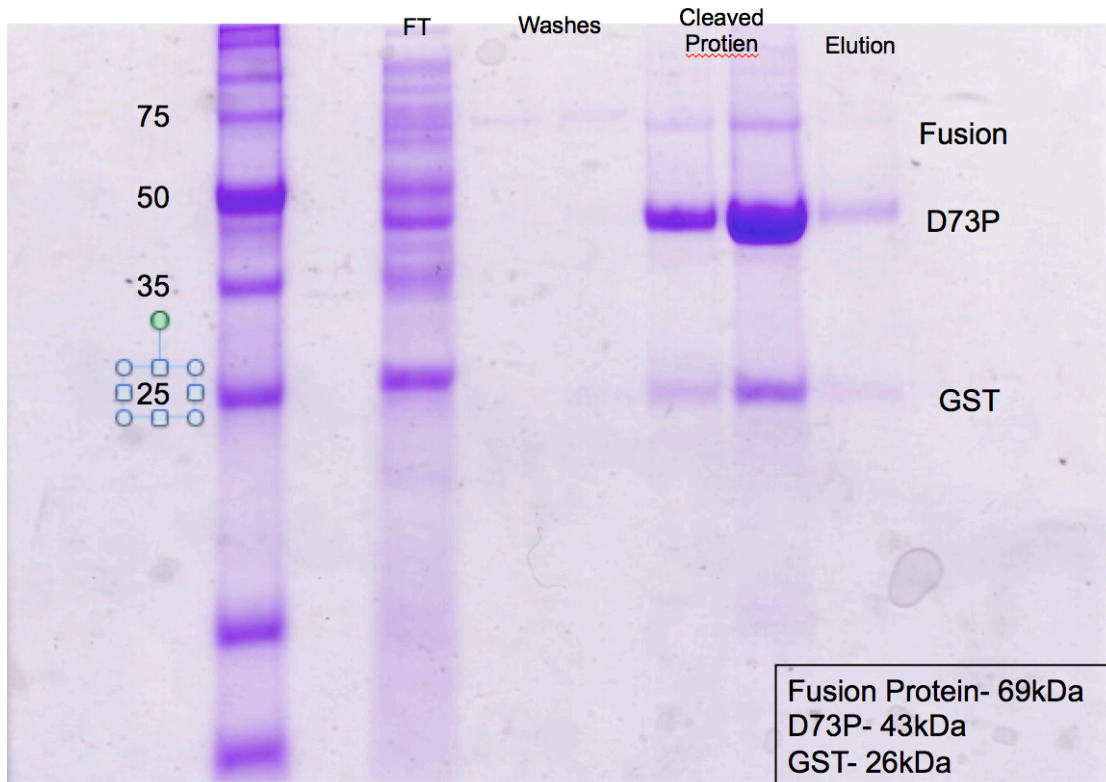


Figure 3.7: SDS PAGE for cis-peptide bond mutant D73P after purification via a glutathione sepharose column. The yield is 1.65 mg protein per liter of cell culture, with the purity ~83.2%

The purity of the purified protein of SDS PAGE sample was determined by using ImageJ software and was quantified to be approximately 83.2%. Due to this purity was not enough for the crystallization trial, Q-sepharose anion exchange chromatography was performed to further increase the purity of the protein sample.

After size exclusion chromatography, the purity of protein sample was found to be approximately 98.7%, with a final yielding of 1.21 mg of fusion protein per liter of cell culture. The protein sample was collect and stored at 4 °C for further characterization.

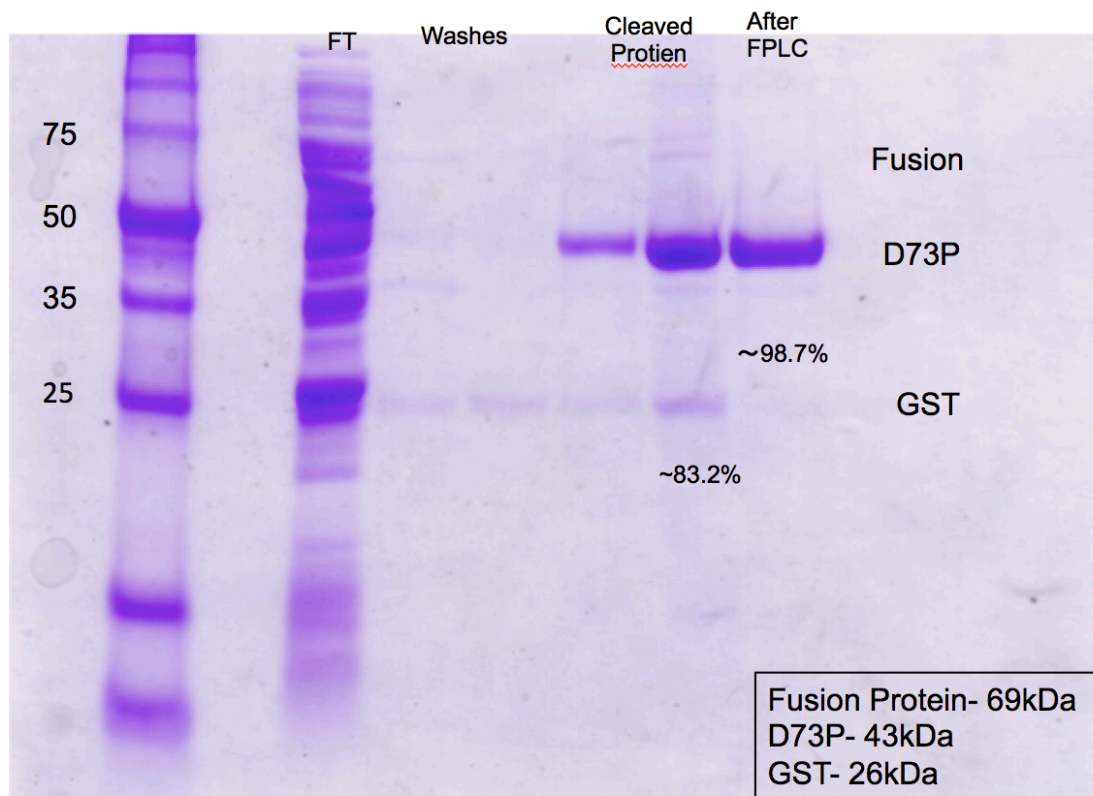


Figure 3.8: SDS PAGE for cis-peptide bond mutant D73P after second purification via Q-sepharose anion exchange chromatography. The yield is 1.21 mg protein per liter of cell culture, with the purity ~98.7%

From the results of the expression and purification of these mutant constructs of PAF-AH, D73G and D73P cis peptide bond mutants have a quiet similar yielding

of ΔPAF-AH. As the assumption we mentioned above, D73G might have changed the cis peptide bond to trans peptide bond while the D73P is assumed to remain the cis peptide bond in this position. Since the D73P mutant construct is assumed to remain the cis peptide bond, the conformation doesn't change a lot, which is corresponding to the similar yield of ΔPAF-AH. However, D73G mutant construct, as a mutant that is supposed to be changed from cis peptide to trans peptide bond, it's yield should have increased due to the reduction of cis-trans isomerization step during the protein expression. The possible explanation of the similar yielding between D73G mutant construct and ΔPAF-AH is the conformation change of cis peptide bond to trans peptide bond greatly destabilizes the protein. Therefore, thought there might not be a cis-trans isomerization step during the expression of D73G mutant construct, the instability of this mutant construct leads to a relatively low protein yielding.

3.3.2 PNPA assay

The specific activity of ΔPAF-AH, D73G and D73P was determined via the application of PNPA as a serine hydrolysis substrate, which was described in section 3.2.6. As Figure 3.9 shows, all constructs were found to have relatively similar enzyme activity. The specific activity values are as follows: ΔPAF-AH= 39.58 μmol/mg·min, D73G= 38.42 μmol/mg·min and D73P= 40.32 μmol/mg·min. The result indicates that site-directed mutation at residues 72nd and 73rd did not affect the enzyme activity

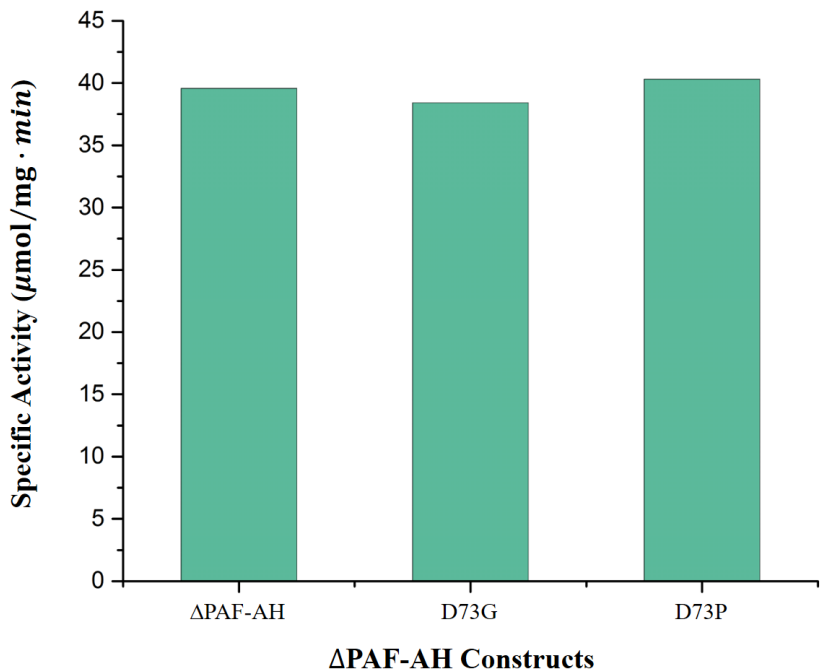


Figure 3.9: Specific enzyme activity of $\Delta\text{PAF-AH}$ and cis-peptide bond mutants D73G and D73P via PNPA assay.

3.4 Conclusions

Presented in this chapter was the expression, purification and characterization of the platelet activating factor acetyl hydrolase. A second glutathione sepharose column incubation was performed to optimize the purification process. In addition to the WT $\Delta\text{PAF-AH}$ expression, purification and characterization, D73G and D73P mutant constructs were made for further study of this rare non-prolyl peptide bond at the same procedure of purification of WT $\Delta\text{PAF-AH}$. These mutants were expressed and purified in the same method as wild type, $\Delta\text{PAF-AH}$. Evaluation of the activity of these two mutant constructs proved there were no significant differences in the

specific activity between wild type ΔPAF-AH and mutant constructs. Similar enzyme activities between wild type and cis-peptide bond mutations point out that this rare non-prolyl cis-peptide bond might have no influence on enzyme activity, consistent with the hypothesis described on Chapter 1.3.

Table 3.2 Yield and purity of protein samples of ΔPAF-AH, D73G and D73P

PAF-AH Construct	Protein Yield (mg/L)	Purity(%)
ΔPAF-AH	1.32	97.5
D73G	1.14	93.1
D73P	1.21	98.7

REFERENCES

1. Tjoelker, Larry W., et al. "Anti-inflammatory properties of a platelet-activating factor acetylhydrolase." *Nature* 374.6522 (1995): 549.
2. Stafforini, D. M., Stephen M. Prescott, and Thomas M. McIntyre. "Human plasma platelet-activating factor acetylhydrolase. Purification and properties." *Journal of Biological Chemistry* 262.9 (1987): 4223-4230.
3. Kilikian, B. V., et al. "Process strategies to improve heterologous protein production in Escherichia coli under lactose or IPTG induction." *Process Biochemistry* 35.9 (2000): 1019-1025.

Chapter 4

CIRCULAR DICHROISM CHARACTERIZATION OF ΔPAF-AH AND CIS-PEPTIDE BOND MUTANT STABILITY

4.1 Introduction

Circular dichroism (CD) is known as the different absorption of left-handed (L) and right-handed (R) circularly polarized light. It is an excellent method for evaluating the secondary structure, folding and binding properties. Because the CD signals can only arise where the absorption occurs, complementary structural informations can be obtained from some spectral regions.

In proteins, the chromophores of peptide bond can usually be absorbed in the region below 240 nm, while absorption of the aromatic amino acid side chains can be observed in the range 260 nm to 320 nm. Moreover, different type of regular secondary structure found in proteins has characteristic CD spectra in the Far UV region (Figure 4.1). There are negative bands at 222 nm and 208 nm for the α -helical protein and negative band at 218 nm can be observed for protein contains well-defined β -pleated sheets. Different from well-folded protein, disordered protein has a low ellipticity at 210 nm and a negative band near 195 nm.

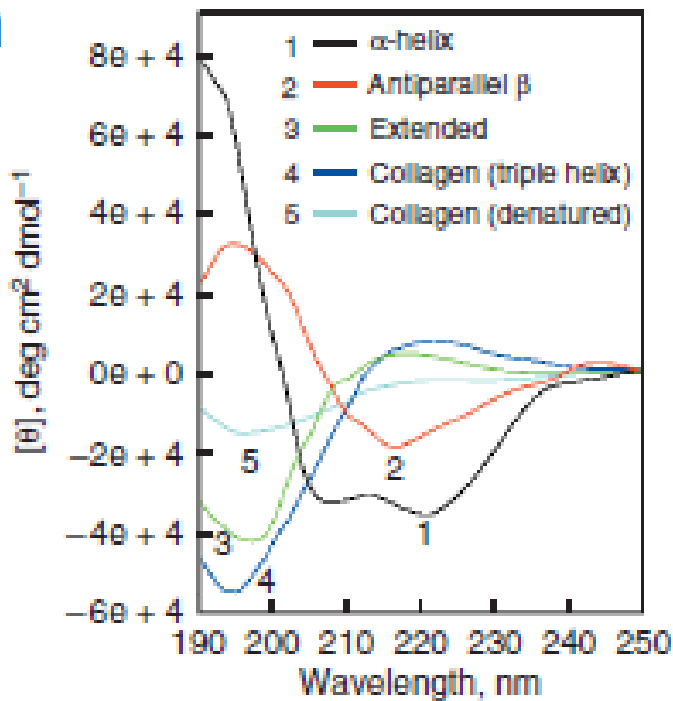


Figure 4.1: Characteristic circular dichroism spectra of secondary structure of protein.

Moreover, CD is also a great technique for following the unfolding and folding of proteins as a function of temperature. As the description above, when protein are folded they often have highly asymmetric secondary structure elements such as α -helices and β -pleated sheets, which have characteristic CD spectra. When the temperature increases, protein starts to unfold to lose these highly ordered structures and the CD bands change. The changes in CD as a function of temperature at specific wavelength, it can be used for determination of thermodynamics of proteins. In this work, this function was performed to test the stability of Δ PAF-AH and cis-peptide bond mutants.

4.2 Methods and Materials

4.2.1 Materials

The material used for the kinetic and structural analysis include sodium chloride, sodium phosphate dibasic anhydrous and sodium phosphate monobasic monohydrate, sodium fluoride were purchased from Fisher Scientific. All other materials for the production of ΔPAF-AH and cis-peptide bond mutants are listed in Chapter 2 and 3.

4.2.2 Determination of secondary structure of ΔPAF-AH

ΔPAF-AH and cis-peptide bond mutants were expressed and purified as described in Chapter 3. The protein samples obtained from FPLC were dialysis overnight into 2 L of running buffer containing 10mM phosphate (6 mM Na₂HPO₄ and 4 mM NaH₂PO₄), 50 mM NaF at pH 7.0 to ensure complete buffer transfer in all samples. Samples were diluted to around 0.1 mg/mL before CD test. Circular dichroism was carried out by using a JASCO Spectropolarimeter in Colburn Laboratory at University of Delaware. During this whole test, temperature was maintained at 20 °C with a Julabo F25 water bath and controlled by a JASCO Peltier Controller. CD spectra were collected in triplicate by using a quartz cuvette with a 1mm path length, a data pitch of 0.5 mM, scanning speed of 50 nm/min, and a response of 4 s. The wavelength range was from 195 nm to 250 nm. Before the measurement, a blank was run of dialysis buffer to automatically correct the baseline.

4.2.3 Circular dichroism thermodynamics determination of melting temperature of ΔPAF-AH

ΔPAF-AH and cis-peptide bond mutants were expressed and purified as described in Chapter 3. The protein samples obtained from FPLC were dialysis overnight into 2 L of running buffer containing 10 mM phosphate (6 mM Na₂HPO₄ and 4 mM NaH₂PO₄), 50 mM NaCl at pH 7.0 to ensure complete buffer transfer in all samples. After overnight dialysis protein samples were concentrated by Amicon Ultra centrifugal filter units (30 kDa molecular weight cut-off, Millipore) at 2000 rpm (Sorvall SH-3000) to a final protein concentration around 0.5mg/mL before CD test. Circular dichroism was carried out by using a JASCO Spectropolarimeter in Colburn Laboratory in University of Delaware. An initial spectra measurement of the protein sample was performed to determine the wavelength that have maximal ellipticity at 20 °C. Then the measurements were performed by using a quartz cuvette with a 0.5 mm path length, a data pitch of 2 °C, temperature slope from 10 to 20 °C, a delay time of 180 s and a response of 2 s. The temperature range was from 10 °C to 90 °C.

4.3 Results and Discussions

4.3.1 Secondary structural analysis

The circular dichroism spectrum was obtained from wild type ΔPAF-AH and cis-peptide bond mutants D73G and D73P. Despite of the automatic deduction of the baseline, the data set still needed further analysis. In order to obtain the mean molar ellipticity per residue, the unit of the ellipticity was converted from the mdeg as CD reported to deg. The concentration of enzyme was calculated in dmol/mL and number of residues would be accounted for. The mean molar ellipticity per residue was performed as a final unit $\text{deg}\cdot\text{cm}^2\cdot\text{dmol}^{-1}$. After this unit conversion, the CD spectrum was shown the mean molar ellipticity per residue at each wavelength.

The CD spectra of ΔPAF-AH, D73G and D73P did not show any obvious differences. Since most of proteins contains both α -helices and β conformation, the spectra show the combination of these two structures. All cis-peptide bond mutant samples remained fully folded, therefore ensure the reliability of the later CD thermodynamics test.

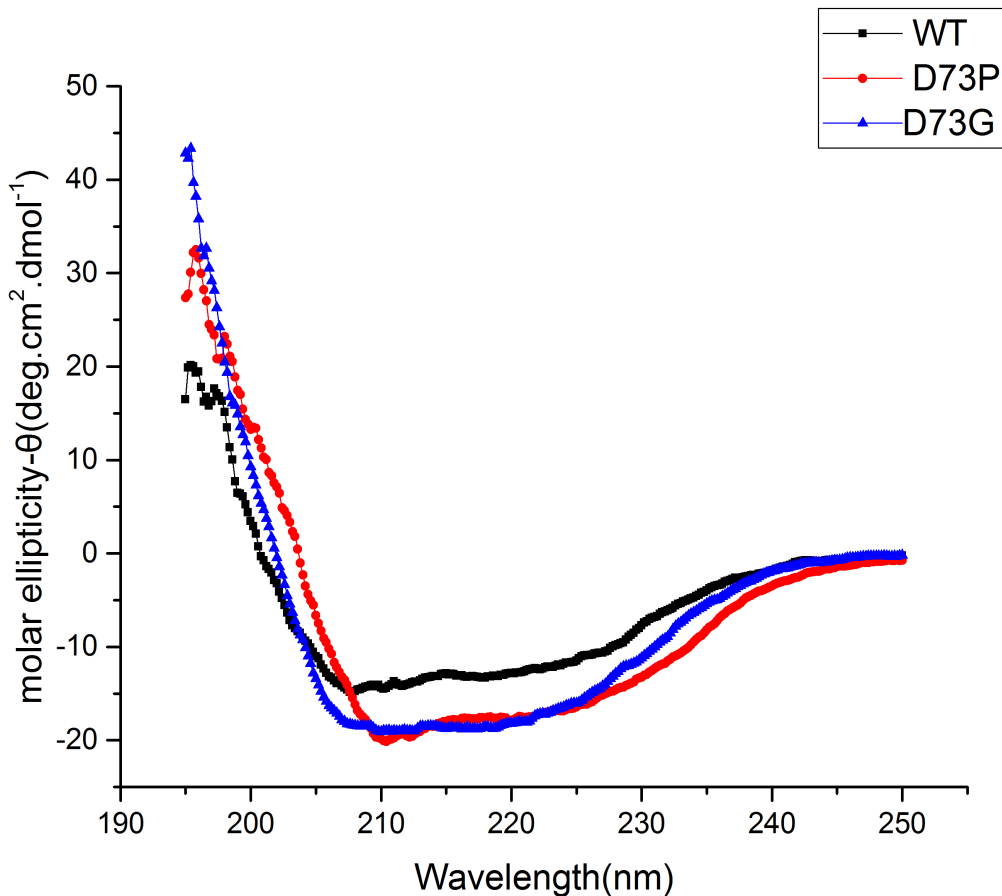
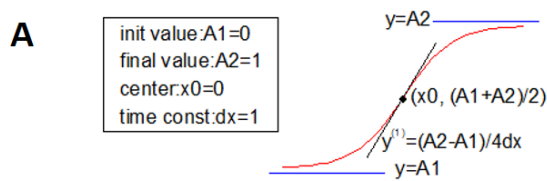


Figure 4.2: Circular dichroism secondary structure analysis of Δ PAF-AH and cis-peptide bond mutants D73G and D73P. Δ PAF-AH is showing in black squares. D73P mutant is showing in red circles and D73G mutant is in blue triangles. No significant changes in the spectrum for any of the constructs.

4.3.2 Determination of melting temperature

The circular dichroism thermodynamics was obtained from wild type ΔPAF-AH and cis-peptide bond mutants D73G and D73P. First the unit of data set was converted to deg·cm²·dmol⁻¹ to determine the mean molar ellipticity per residue at each temperature. After conversion, the CD thermodynamics data was fit by using the sigmoid curve vs. Boltzmann function of Origin version 2016 for Windows. The melting temperature was obtained from this nonlinear fitting.



B

$$y = \frac{A_1 - A_2}{1 + e^{(x-x_0)/dx}} + A_2$$

Figure 4.3: (A) Sample curve of sigmoid curve vs. Boltzmann function (B) Formula of sigmoid curve vs. Boltzmann function

Two samples of wild type Δ PAF-AH were run under the temperature slope of 15 °C/h and 20 °C/h separately at wavelength 222 nm. The melting temperature T_m calculated from CD thermodynamics data set was 77.7 °C and 81.0 °C.

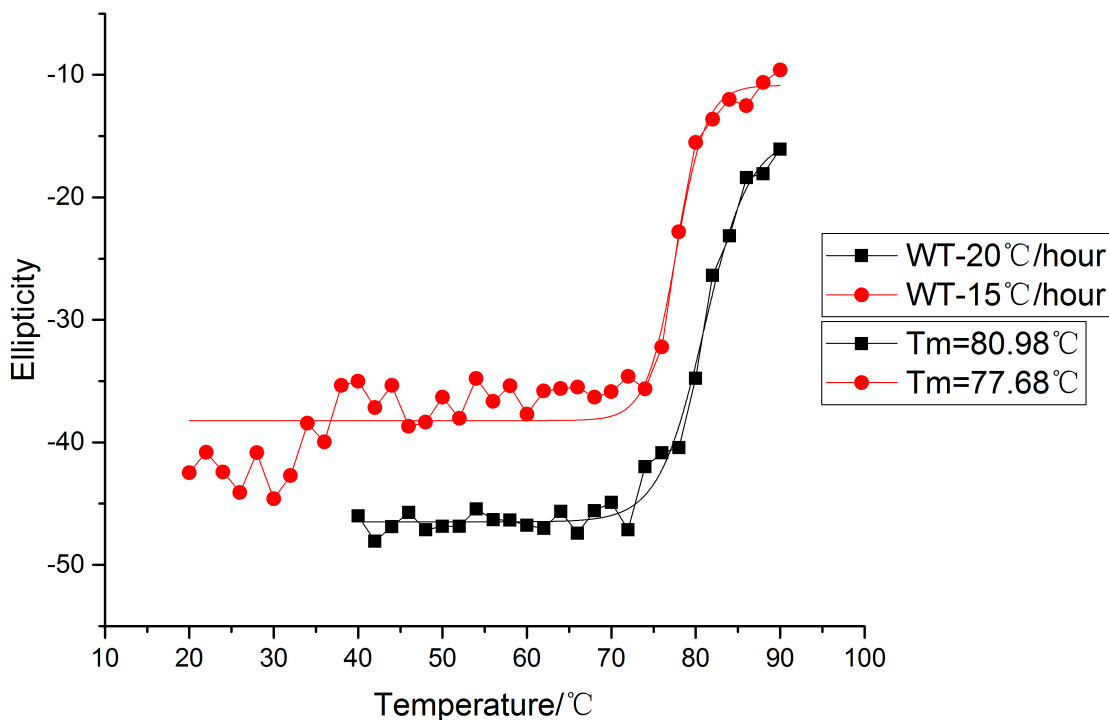


Figure 4.4: Circular dichroism thermodynamics analysis of Δ PAF-AH. The melting temperature was calculated via Origin 2016 software for windows. Calculated T_m was 81.0/77.7 °C.

Two samples of cis-peptide bond mutant D73P were run under the temperature slope of 10 °C/h separately at wavelength 222 nm. The melting temperature T_m calculated from CD thermodynamics data set was 72.7 °C and 75.20 °C.

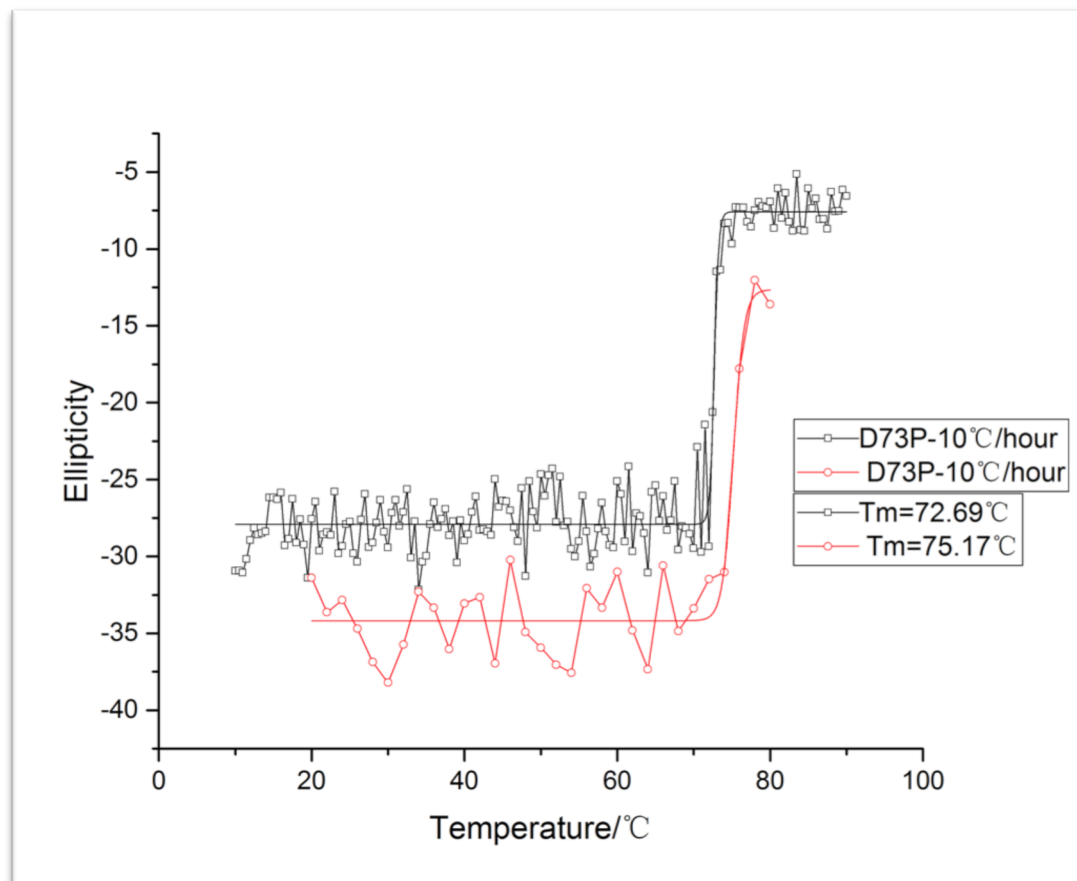


Figure 4.5: Circular dichroism thermodynamics analysis of cis-peptide mutant D73P. The melting temperature was calculated via Origin 2016 software for windows. Calculated T_m was 72.7/75.2 °C.

Two samples of cis-peptide bond mutant D73G were run under the temperature slope of 10 °C/h and 20 °C/h separately at wavelength 222 nm. The melting temperature T_m calculated from CD thermodynamics data set was 62.6 °C and 60.3 °C.

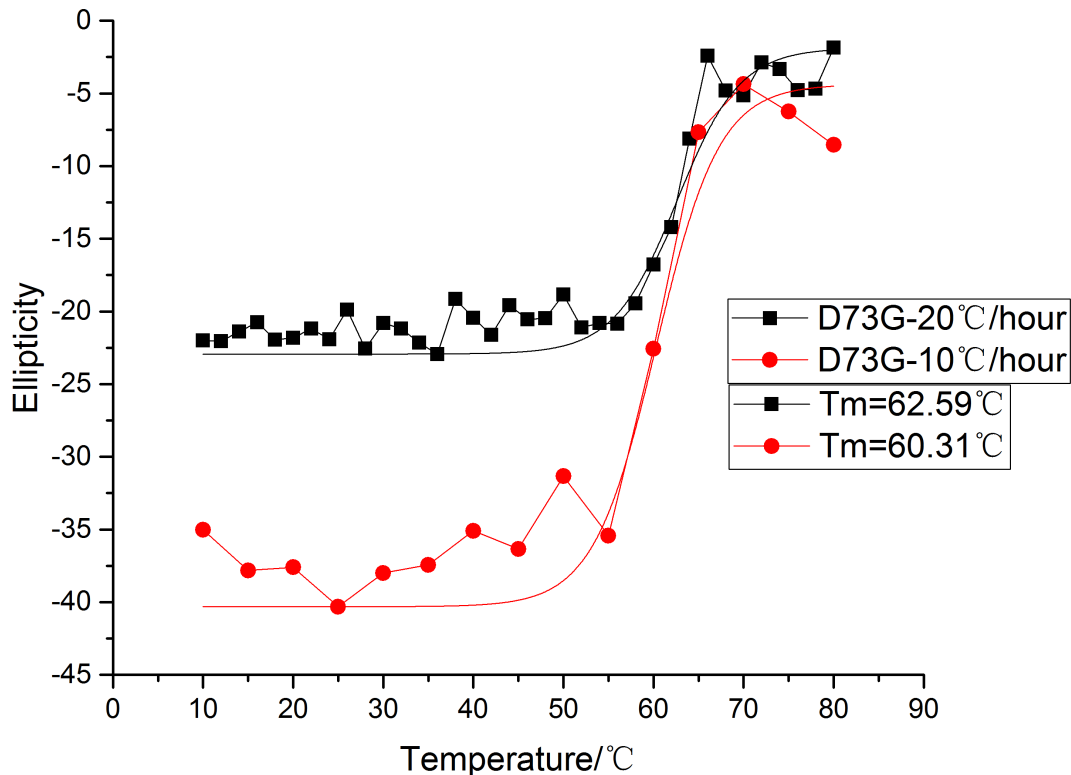


Figure 4.6: Circular dichroism thermodynamics analysis of cis-peptide mutant D73G. The melting temperature was calculated via Origin 2016 software for windows. Calculated T_m was 62.6/60.3 °C.

4.4 Conclusions

Presented in this chapter was the structural characterization and stability of the high-purity platelet activating factor acetyl hydrolase via CD instrument. The CD spectra of ΔPAF-AH, D73G and D73P did not show any obvious differences, indicating that all cis-peptide bond mutant samples remained fully folded. Considering the similarity of CD spectra about secondary structure between wild type and cis-peptide bond mutations, this non-prolyl cis-peptide bond might have little influence on protein folding.

Though protein samples after first purification (glutathione sepharose column) can also be performed on CD thermodynamics (protein purity range from 76% – 82 %), in order to increase the reliability of data set, we use the high purity of the protein samples (protein purity range from 93% - 99%). The detailed information about the wild type construct ΔPAF-AH and two cis-peptide bond mutants are shown in the Table 4.1.

The melting temperature of D73G greatly decreases compared to WT ΔPAF-AH. The possible explanation of the instability of this mutant is that this cis-peptide bond might have been changed to trans configuration, therefore the structure of PAF-AH is damaged based on the hypothesis that it maintains the binding of LDL. However, there is still not direct evidence to prove that this position is changed to trans configuration. A crystallization trial is essential for the structure analysis of this mutant. The T_m of D73P also shows a slightly decline. Since the Asp-73 was changed to proline, the structure might be rigid due to the sidechain of proline. For this reason, this mutant cannot adjust well during the temperature change, which might lead to the thermodynamic instability of this mutant.

Table 4.1 Protein yield, purity and melting temperature after second purification of ΔPAF-AH and cis-peptide bond mutants.

PAF-AH construct	Yield(mg/mL)	Purity (%)	T_m (°C)
ΔPAF-AH	1.32	97.5	81.0/77.7
D73G	1.14	93.1	62.6/60.2
D73P	1.21	98.7	72.7/75.2

REFERENCES

1. Kelly, Sharon M., Thomas J. Jess, and Nicholas C. Price. "How to study proteins by circular dichroism." *Biochimica et Biophysica Acta (BBA)-Proteins and Proteomics* 1751.2 (2005): 119-139..
2. Holzwarth, G., and P. Doty. "The ultraviolet circular dichroism of polypeptides1." *Journal of the American Chemical Society* 87.2 (1965): 218-228.
3. Miles, Andrew J., and B. A. Wallace. "Synchrotron radiation circular dichroism spectroscopy of proteins and applications in structural and functional genomics." *Chemical Society Reviews* 35.1 (2006): 39-51.
4. Greenfield, Norma J. "Using circular dichroism spectra to estimate protein secondary structure." *Nature protocols* 1.6 (2006): 2876-2890.
5. Greenfield, Norma J. "Using circular dichroism collected as a function of temperature to determine the thermodynamics of protein unfolding and binding interactions." *Nature protocols* 1.6 (2006): 2527-2535.

Chapter 5

CONCLUSION AND FUTURE DIRECTION

The work presented here contributes to a better understanding of the non-prolyl cis-peptide bond in human plasma PAF-AH. Based on the hypothesis described in Chapter 1, Two site-directed mutants, D73G and D73P, were made with the goal of studying the function of this non-prolyl cis-peptide bond. The comparison of enzyme activity between wild type and two mutants was performed by PNPA assay. There were no functional differences between them, indicating the cis-peptide bond does not play a role in enzyme activity.

The CD secondary structure characterization also points out that the two mutants studied were both folded well during expression and purification, eliminating the possibility that this cis-peptide bond may have a influence on protein folding.

However, we can see there is an obvious decrease of protein stability for these two mutants via the decline of T_m . The D73G mutant had a significantly decreased thermal stability based on a denaturation characterization using CD. Although the D73P mutant was assumed to be in cis configuration, its stability was also reduced albeit to a lower extent, based on a slightly elevated T_m compared to the wild type enzyme.

Moreover, high purity and well-folded protein samples of two mutant constructs were successfully made, which is a necessary step to pursue crystallization trials and subsequent structure determination.

By now, there is no direct evidence to prove the hypothesis that non-prolyl cis-peptide bond play a role in maintain of LDL binding. Therefore, a high-resolution crystal structure is needed for further exploration about its function. Even following the successful future crystal structure of the D73G mutant which may show that this position has been changed to a trans configuration, the correlation between this cis-peptide bond and LDL binding would still not be completely proven. During the structure determination for these two mutants, a molecular dynamics computational calculation for the energy barrier between the wild type and cis-peptide bond mutants can be performed to get a better understanding of these configurations.

Appendix

PERMISSION LETTER

Graph Citation Permission of your Paper Inbox x

 **Shilin Xie** <slxie@udel.edu> Jul 11 (3 days ago) 
to amyand

Hi Amy,

I am a master student at University of Delaware in the U.S. I am working on my thesis and I read your paper "Native State Proline Isomerization: An Intrinsic Molecular Switch". It is a great work! Therefore, I wonder if I can use your graph in my thesis introduction. My thesis won't be published.

Thank you so much!



 **Amy Andreotti** <amyandreotti@me.com> Jul 11 (3 days ago) 
to me

Dear Shilin,

Thanks of being in touch. I'd be delighted for you to use the figure, if the thesis (or any part of it) were to ever be published I think the only thing you'd have to worry about it the copyright of the journal. Good luck with your defense.

All the best,
Amy Andreotti

*Amy H. Andreotti, Ph.D.
Roy J. Carver Chair in Biochemistry
Roy J. Carver Department of Biochemistry Biophysics & Molecular Biology
Iowa State University*

*4208 Molecular Biology Building
Ames, IA 50011
(515)294-4953
amyand@iastate.edu*



Graph Citation of your Paper

Inbox x



Shilin Xie <slxie@udel.edu>

to alexandre.debr.

Jul 11 (3 days ago)

Hi Alexandre,

I am a master student at University of Delaware in the U.S. I am working on my thesis and I read your paper "Cis–trans peptide variations in structurally similar proteins". It is a great work! Therefore, I wonder if I can use your graph in my thesis introduction. My thesis won't be published.

Thank you so much!



Alexandre de Brevern

Jul 12 (2 days ago)

to me

Hello

With great pleasure. And feel free to sent me your thesis if you have the right to do

Sincerely

